Forming Behavior of Paperboard in Single Point Incremental Forming

Philipp Stein, Wilken Franke, Magnus von Elling, and Peter Groche *

An increased demand for sustainable materials has led to intensive research in the field of three-dimensional paperboard forming. To date, this work has focused on forming processes with shape-giving tools. However, individual shapes are often required, especially for large-format products. Incremental forming can be used in metal processing for small batches. In this article, the technology of incremental forming is transferred to paperboard. The results showed that elevated moisture content and a superimposed counter pressure significantly increased the forming limits. In addition, the use of polymer layers increased the shape accuracy. An extended understanding of the underlying mechanisms was achieved by analyzing the forming behavior. In uniaxial and biaxial characterization tests the influence of the moisture content on the forming behavior was investigated with conditions relevant for incremental forming. It was found that the bulge test is suitable to determine the most suitable moisture content regarding the forming limits and the spring back behavior in incremental forming. In addition, it was observed that the bearable elongations during the incremental forming of paperboard are significantly higher than in the established characterization tests. The reason for this is a compression of the fiber network during forming.

Keywords: Paperboard; Incremental forming; Spring back; Mechanical testing; Forming mechanisms

Contact information: Institute for Production Engineering and Forming Machines – PtU, Technische Universität Darmstadt, Otto-Berndt-Straße 2, 64287 Darmstadt, Germany;
** Corresponding author: groche@ptu.tu-darmstadt.de*

INTRODUCTION

In addition to the ongoing problem of climate change, one of today's key issues is the pollution of oceans by plastics. Jambeck *et al.* (2015) determined the annual input of plastic into the oceans as between 4.8 and 12.7 million tons in 2010. Because the degradation of plastics takes up to 400 years (Merkl *et al.* 2015), large garbage patches accumulate in the oceans, which contaminate marine organisms (Lebreton *et al.* 2018). To stop the pollution, closed loop recycling systems are required. However, even if the plastic waste gets collected, it is often incinerated. In Germany, for example, 99 % of used plastics are collected, which corresponds to 5.877 million tons. However, 3.140 million tons of those are energetically recycled, *i.e.*, incinerated (Umweltbundesamt 2016). This procedure results in the release of harmful CO_2 from fossil sources into the environment. Another approach to reduce the plastic waste is the replacement of polymer-based by climate-neutral and sustainable paperboard products. In contrast to plastics, uncoated paperboard, mainly consisting of wood fibers, is degraded in the environment after a few weeks without leaving harmful substances (Sridach *et al*. 2006). While paperboard products with simple geometries like folding boxes are frequently used, complex three-dimensional components (*e.g.*, egg boxes) are manufactured by pulp molding and thus have poor surface quality and strength (Hauptmann and Majschak 2011). The associated poor surface quality and component strength compared to polymer-based components results in complex shaped paper products that are not competitive with polymer products. In order to make paper competitive in the field of complex formed components, some forming processes used in metal processing have been adapted to paperboard. Conventional deep drawing (Hauptmann 2010; Lohse *et al.* 2010), press forming (Golzar and Ghaderi 2009; Leminen *et al.* 2013), and hydroforming (Huttel and Groche 2014; Linville and Östlund 2016) have been intensively investigated. These studies focused on understanding and improving the forming behavior of paperboard. The results show that the forming limits as well as the component quality of paperboard can be improved by:

- An elevated moisture content (Scherer 1935; Rhim 2010),
- Enhanced tool temperatures (Tanninen *et al.* 2014; Wallmaier *et al.* 2016),
- A sufficient calibration time (Tanninen 2015),
- A trajectory blank-holder force (Hauptmann *et al.* 2016a; Müller *et al.* 2017),
- An in-process steam application (Franke *et al.* 2018),
- A superimposed counter pressure (Groche and Huttel 2016), and
- A superimposed ultrasonic vibration (Löwe *et al.* 2017a).

A closer look at the fiber network and the forming mechanisms is required to understand why the listed parameters extend the forming limits. This knowledge is required to analyze the forming behavior of paperboard in characterization tests and in incremental forming. Therefore, the forming mechanisms are described in detail below, followed by a selective introduction to the incremental forming.

Forming Mechanisms

Figure 1 shows the different forming mechanisms for paperboard (Vishtal and Retulainen 2012; Groche and Huttel 2016). For reasons of clarity, the mechanisms are presented separately, although the forming is usually based on a combination of the individual mechanisms. Various approaches for influencing the forming mechanisms with a view to the mentioned improvements of formability are described afterwards.

Neither the schematic depiction nor the subsequent discussion considers filler materials. Especially in recycled paperboard, there are fillers between the fibers that influence the material behavior. Because the variation and concentration of fillers (*e.g.*, printing residues or minerals) is almost unlimited, most scientific studies on the forming behavior of paperboard were carried out on fresh fiberboard with a clear network structure like depicted in Fig. 1 a).

Fiber network strength by hydrogen bonds

Except for the mechanism “elongation”, the forming of paperboard is primarily based on a fiber movement. Hydrogen bonds (represented by blue dots in Fig. 1) are responsible for the inter-fiber connection and the fiber network strength (Putz 2013). Thus, weakening the hydrogen bonds during the forming process enables fiber movement, which increases the extensibility. The weakening can easily be adjusted by increasing the moisture content (Haslach 2000). However, the improvement of the forming that can be achieved as a result of increased moisture content is only possible to a limited extent; in tensile tests, there are higher elongations at break at 15 % than at 20 % moisture content (Huttel 2015).

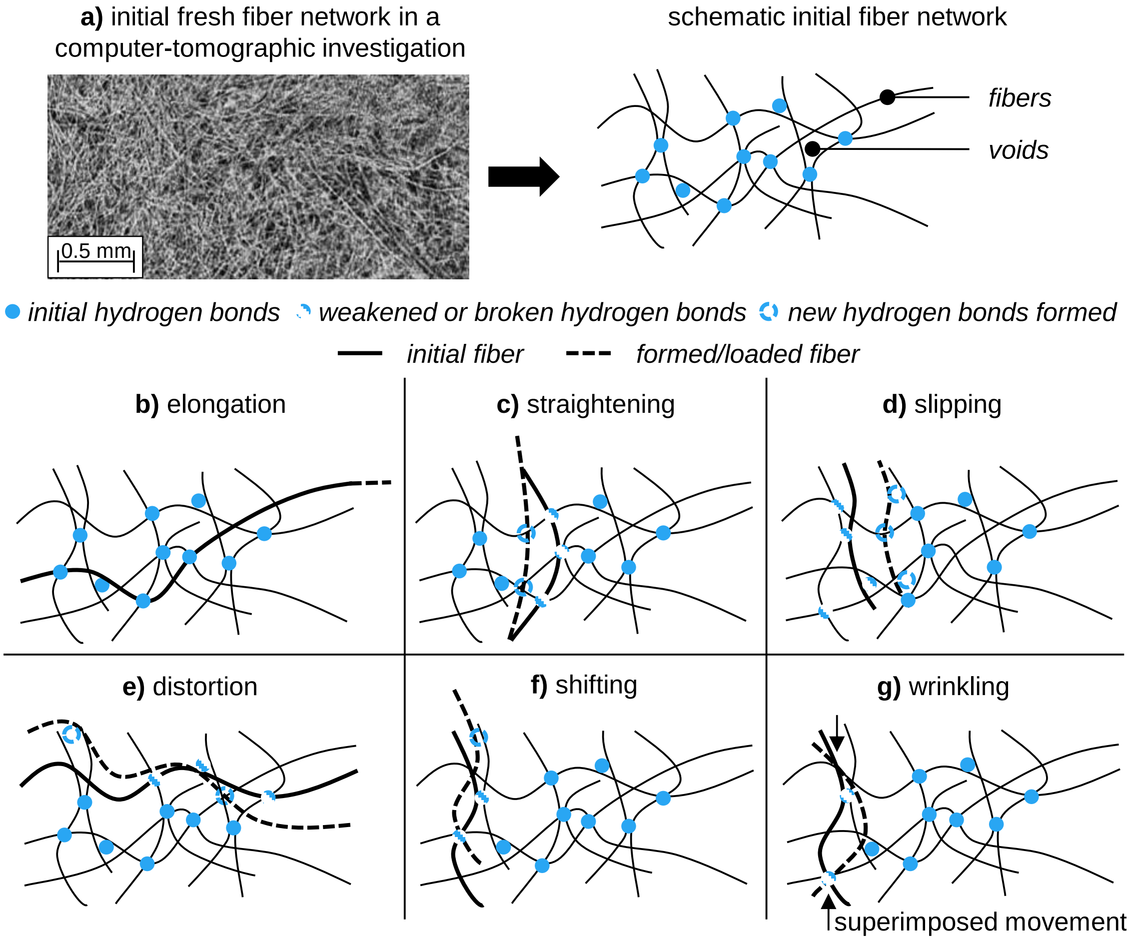

Fig. 1. Schematic depiction of the forming mechanisms of paperboard; in reference to Vishtal and Retulainen (2012) and Groche and Huttel (2016)

Because paper is hygroscopic (Rhim *et al*. 2006), there is a constant exchange of moisture between paper and the ambient medium. To eliminate the influence of a varying moisture content onto the forming behavior, a multitude of the conducted investigations regarding the three dimensional forming were performed in an air-conditioned environment. Beside a limited applicableness to industrial conditions, this leads to a restriction regarding the maximal moisture content since the hygroscopic moisture adsorption is limited (Bedane *et al.* 2014). Thus, the moisture content was set to about 10% in most previous investigations of the three dimensional forming of paperboard. Nevertheless, higher moisture contents are known to improve the forming limits (Huttel 2015).

Influence of temperature on the forming mechanisms

While the hydrogen bonds are influenced by water between the fibers (voids, *cf.* Fig. 1), the elongation of the fibers themselves is also influenced by water embedded in the fibers (Östlund 2005). Additionally, the extensibility can be increased by softening the ingredients by heat input (Salmén 1993; Bos *et al.* 2006a). Salmén (1993) determined that the required temperature to soften the main ingredients, namely lignin, hemicellulose, and cellulose, is dependent on the moisture content. At 0% moisture content, the required temperature for the mentioned ingredients is approximately 200 °C.

For lignin, the minimum temperature required is reduced to a constant value of 100 °C at moisture contents greater than 20 %. The softening temperature for hemicellulose and cellulose also decreases while the moisture content increases. At a moisture content of 30 % hemicellulose already softens at room temperature. The softening temperature of cellulose, however, decreases almost constantly with increasing moisture content and reaches 50 °C at 40 % moisture content.

Extending the extensibility by counter pressure

A further approach to increase the extensibility of the fiber network is to apply a counter pressure, as described by Groche and Huttel (2016). In order to apply a counter pressure of 2 N/mm², they placed the paperboard between two steel sheets. Due to the significantly higher forming resistance of the steel sheets, a force is applied perpendicularly to the paperboard plane. They assume that, as a result of the perpendicular force, a hydrostatic pressure is applied, which leads to extended forming limits. To confirm this assumption, Stein *et al*. (2018) developed a test stand and carried out tensile tests under hydrostatic pressure. There was no significant increase in extensibility after applying hydrostatic air pressure (8 and 32 bar) in the tensile test chamber. This means that, contrary to metals (Yajima *et al.* 1970), a hydrostatic pressure does not affect the maximum elongation of paperboard under all circumstances. Because the application of the counter pressure by steel sheets also leads to a compression of the samples, Stein *et al*. (2018) conducted tensile tests on samples that had been compressed before the tensile test.

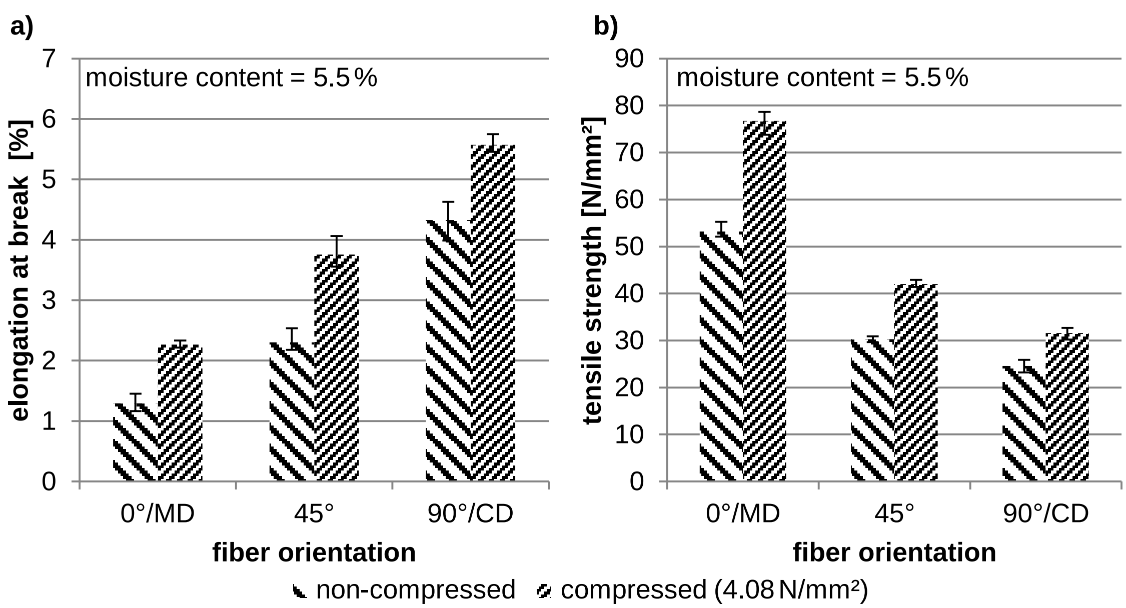

Fig. 2. Mechanical properties of non-compressed and compressed samples, determined in a conventional tensile test at 5.5 % moisture content (Stein *et al*. 2018), with permission of the organizing committee

As shown in Fig. 2 a, the elongation at break of pre-compressed samples (contact stress = 4.08 N/mm²) is increased by up to 74.8 % at a moisture content of 5.5 % in MD (preferred fiber direction, abbreviation: MD, 0°). In 45° fiber orientation, the increase of 62.75 % is slightly lower. In CD (transverse to MD, abbreviation: CD, 90°), however, the increase is only 28.70 %. Independently from the fiber orientation, the sample thickness is reduced from 0.53 mm to 0.45 mm at 5.5 % moisture content and from 0.62 mm to 0.44 mm at 20 % moisture content. The increased initial thickness at 20 % moisture content is due to swelling.

The reason for the lower increase in CD is based on a different forming mechanism compared to MD. During the pre-compressing, fibers are pressed into the existing voids. Hence the density of the sample increases (Vainio and Paulapuro 2007). Pushing the fibers into the voids can best be described with the "wrinkling" mechanism shown in Fig. 1 g). During the subsequent tensile test, the pressed-in fibers serve as an expansion reservoir, which significantly increases the bearable elongation. According to Fig. 1 c), this effect can be described by the "straightening" mechanism. Because the fibers must be aligned along the load direction for this, there is a clearer increase in MD than in CD or 45° fiber orientation. This tendency is also valid with an increased moisture content of 20 %. However, the increase is reduced to values of 24.64 % in MD and 10.71 % in CD. The lowered increase can be explained by the embedded water in the fibers and voids which prevents a “wrinkling” of the fibers into the voids since water is, contrary to air, incompressible.

As depicted in Fig. 2 b), the tensile strength is also increased by the pre-compressing process. As for elongation at break, the increase is highest in MD. The increase in tensile strength is explained by fewer voids and thus an increased contact area between the fibers, which enables the forming of more hydrogen bonds (Vainio and Paulapuro 2007) and leads to increased strength in the fiber network. Hauptmann *et al*. (2015) determined a similar behavior for paperboards with different fiber treatments resulting in different volumes of the voids. In contrast to the elongations at break, the tensile strength rises stronger at 20 % moisture content due to the pre-compressing than at 5.5 % moisture content. This behavior is explained by the higher initial thickness (0.62 mm) of the moistened samples. In consequence, the distance between the fibers is higher compared to a moisture content of 5.5 % and thus fewer hydrogen bonds exist. Nevertheless, due to the pre-compressing process the samples are pressed to 0.44 mm with the result of a smaller distance between the fibers, which enables more hydrogen bonds to be formed at increased moisture content.

Increased shape accuracy by adapted process parameters

In addition to increasing forming limits, there have been efforts to enhance the shape accuracy of three dimensionally formed paperboard parts, as customers perceive inaccuracies as poor quality. Paperboard forming results in three main shape inaccuracies, namely spring back, shrinkage, and wrinkling.

Spring back is based on mechanical energy saved in the fiber network due to elastic elongations. Tanninen *et al*. (2016) showed that a dwell time of 2 seconds in the mold in combination with elevated tool temperatures (160 °C) reduces spring back. This can be explained by the new formation or reinforcement of hydrogen bonds by drying after the forming process. Because paperboard has a distinctive creep behavior (Allaoui *et al*. 2009), a dwell time enables the fibers to relax. With regard to the forming mechanisms, this means that fibers can continue to elongate or relocate. Because there is no further deformation, stresses between the fibers and, consequently, spring back are reduced.

In contrast to spring back, shrinkage is based on drying (Östlund 2005). However, the shrinkage behavior of paperboard during three dimensional forming processes has not been investigated, partly because it is difficult to distinguish between spring back and shrinkage within forming processes. For example, a longer dwell time influences the shrinkage rate after the process by improved drying within the mold.

The third shape inaccuracy, wrinkling, results from an excess of material and is observed in forming processes with in-plane compressive stresses. For example, in deep drawing this comes along with a material surplus in the flange area during the process. In metal forming this leads to tip formation at the outer edge as well as thickening in radial direction in the flange area due to the dislocation movement. Because no dislocations move within the paperboard network (Groche and Huttel 2016), the excess material leads to an overlapping of the fiber layers (Hauptmann and Majschak 2011). Hauptmann *et al*. (2016a) succeeded in reducing the resulting wrinkles through targeted control of the blank holder force. According to the shaping mechanisms, this is only possible if there are sufficient voids into which the excess fibers can be pressed. An extension of mere pressing was introduced by Löwe *et al*. (2017a). They superimposed an ultrasonic oscillation on the deep drawing process and thus reduce forming forces, improve stiffness and compress the wrinkles (smooth surface) (Löwe *et al*. 2017b). Higher temperatures occur in the specimens, making the ingredients become softer. Furthermore the fiber movement is facilitated by the vibrations. In consequence, penetration of fibers into the voids by “wrinkling” as well as a material compression by “slipping” (voids get closed) is supported.

Anisotropic forming behavior

While various investigations pursued different approaches to improve the forming limits, the anisotropic material behavior of paperboard led to shape deviations between the MD and the CD in all investigations. The anisotropic material behavior is a consequence of the manufacturing process. When the paperboard fibers are flushed onto the sieve they are primarily getting aligned parallel to the flux (Bos *et al.* 2006b) which leads to a different forming behavior with regard to the fiber orientation. The strength in MD is significantly higher than in CD, while the elongations at break are significantly higher in CD than in MD. Franke *et al*. (2018) determined in tensile tests elongations at break values 3.16-times higher in CD than in MD at 5 % moisture content and 2.769-times higher at 20 %. To understand the mechanism a closer look to the fiber network is required, as depicted in Fig. 3.

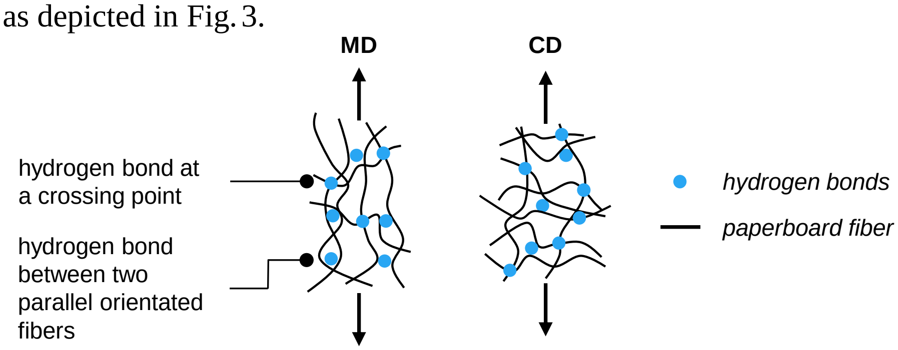

Fig. 3. Schematic depiction of the fiber network in fiber preferred direction (MD) and perpendicular to that (CD)

When a sample is pulled with fibers mostly orientated in tensile direction (MD), more fibers are loaded parallel to their orientation. In contrast, in the CD the fibers are loaded to a greater degree perpendicularly to their longitudinal orientation. Comparing the fibers with conventional ropes, it becomes obvious that the required force to elongate the fibers lengthwise is significantly higher than the force perpendicularly to this direction. Additionally, the hydrogen bonds located between the fibers (cf. Fig. 3) are less influenced when pulling in the MD. The reason for this is that the distance between the loaded fibers remains constant. In contrast, in CD the distance increases and thus the hydrogen bonds between the fibers are weakened or broken, which results in less network strength but higher bearable elongations. The hydrogen bonds located at crossing points of MD- and CD-fibers do not influence the anisotropic forming behavior. Vishtal and Retulainen (2012) additionally explain that more curled fibers are located in the CD. Straightening the curled fibers can be regarded as an elongation buffer, which means that higher elongations can be endured in CD than in MD.

The drying section in the manufacturing process of paperboard further increases the anisotropic behavior. While the fibers are stretched in MD by the paper machine and thus shrinkage is suppressed, shrinkage in CD is only influenced by the low frictional force between paper and drying rollers. In consequence, higher residual stresses occur in CD than in MD, which affects the mechanical properties. (Bos *et al.* 2006c)

Incremental Forming

Most of the above mentioned investigations regarding paperboard forming were conducted with full shape-giving tools (deep drawing, press forming) or partially shape-giving tools (hydroforming). As a consequence, shape variations lead to high tooling costs. In mass production, as with packages, these costs are compensated by the high number of products produced. However, paperboard also offers opportunities for sustainable application in the field of furniture, car panels (Pflug *et al.* 2002) or as facade elements (Schabel 2017). While moisture resistance can already be achieved by chemical modifications or coatings (Rhim *et al.* 2007; Havimo *et al.* 2011), there is no three-dimensional forming technology available for manufacturing large-scaled paperboard products. Because furniture and facades are often designed individually for reasons of recognition, an economical process is required for small batches. A technology which fulfills these requirements is incremental sheet forming (Jeswiet *et al.* 2005). The incremental forming without any die can be divided into the single point incremental (Fig. 4 a) and the incremental forming with counter tool (Fig. 4 b). The shape variants are limited only to the degrees of freedom of the CNC machines or robots used. Most machines provide at least three degrees of freedom. Thus, the forming tools can run any horizontally oriented tool path, as exemplarily depicted in topside views in (Fig. 4 c). The three dimensional shape is created by a radial (Δr) and a vertical infeed (Δz). The infeed can be made after each rotation (see Fig. 4 a) or continuously, *e.g.* through a spiral tool path.

A further advantage of the incremental forming towards common forming technologies is the reduction of the forming force due to the localized forming process (Bambach 2007). This enables forming of large scaled parts with a relatively low machinery investment.

Because incremental forming is primarily used for small batches and allows almost countless process variants (machining path, tool diameter, speed, *etc.*) a prediction of the forming limits is nearly impossible. Therefore, it is common to determine the forming limits with the aid of a common geometry and a given tool set. The maximum achievable flank angle α (cf. Fig. 4 a) gives a measure for the formability (Hirt *et al.* 2004). For metals values between 40 and 76 ° are possible when forming a truncated cone (Behera *et al.* 2017). Investigations regarding the maximal flange angle of paperboard for incremental forming are not known. Stein *et al*. (2017) already used the degrees of freedom in a single point incremental forming process to compensate the anisotropic material behavior of paperboard by an adapted process strategy. However, so far neither the forming limits of paperboard in incremental forming have been determined nor the shape accuracy depending on different process parameters.

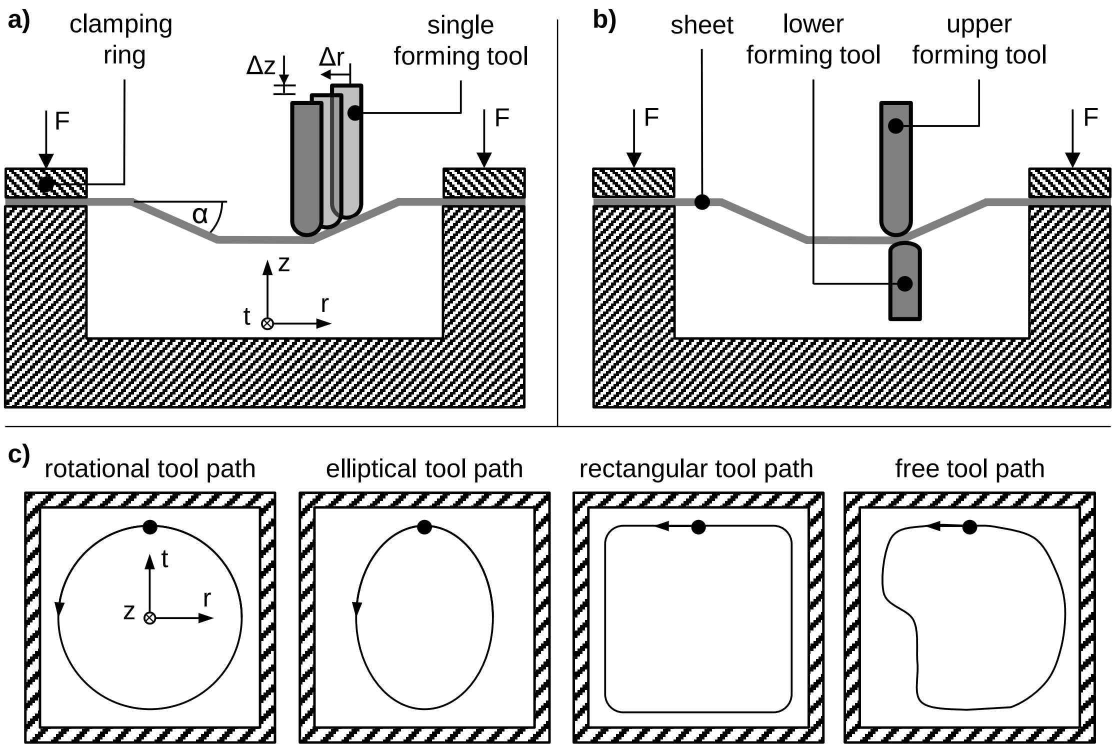

Fig. 4. Variants of incremental forming without additional dies a) single point incremental forming; b) two point incremental forming; c) topside view of different possible tool paths; (drives and units are not depicted)

Objectives

There is a need for a cost-efficient, individual forming process for paperboard. Therefore, this paper investigates the incremental forming of paperboard. In addition to process development, the aim is to determine whether known optimization parameters from conventional paperboard forming processes can be adapted to incremental forming.

Because the design of incremental forming processes is still primarily based on the trial and error principle, the aim is to reduce the scope of experiments by means of standardized material characterization tests. Based on the fact that mainly plane and biaxial stresses occur during incremental sheet forming, tensile and bulge tests are performed. Additionally, a comprehensive understanding of the process is to be achieved. For this purpose, the determined process limits and the shape deviations are analyzed taking into account the forming mechanisms.

EXPERIMENTAL

The following discussion describes the setups and the procedures in the used characterization tests as well as the applied evaluation methods. For a better understanding, the descriptions are divided into the sections “tensile test” and “pneumatic bulge test”. The new developed test rig for the incremental forming of paperboard is described in the section “test rig for incremental forming”.

In all tests, the industrial fresh fiber paperboard Trayforma® with a grammage of 390 g/m² (afterwards: fresh fiber paperboard) from StoraEnso, Finland was used. This paperboard has a three-layer fiber construction with a chemi-thermomechanical pulp in the core. The data listed in Table 1 are from the public StoraEnso data sheet. (Datasheet Trayforma 2018).

Table 1. Material Data for the Used Fresh Fiber Paperboard

Parameter	Value
thickness	550 µm
bending resistance L&W 15° MD/CD	790 / 300 mN
brightness D65/10, top	84 %
surface smoothness, Bendtsen, top/reverse	700 / 800 ml/min
stretch CD	6.0 %

Tensile Test

Tensile tests for paperboard are standardized in DIN EN ISO 1924-2 (2009). However, the required sample geometry (rectangular strip) is not suitable because no homogeneous stress-strain distribution is given (Huttel 2015). Based on the bone-shaped geometry, as used for metals DIN 50125 (2009), a new specimen geometry has been developed for paperboard testing (Huttel 2015). Due to the more uniform stress and strain distributions in the analysis area of the specimens, the fracture occurs almost exclusively in the middle of the newly shaped samples. This improves observation and evaluation of the tests. Based on its advantages, this geometry was used in the present work. To exclude the influence of machine elasticity (ZwickRoell 100), the elongations were determined by an external optical measurement system (videoXtens®).

To determine the moisture content that leads to the highest elongations at break, a variation from 4.5 up to 25 % moisture content was conducted. To adjust the moisture content, the specimens were dried, based on DIN EN ISO 287 (2009). To consider the fiber orientation of the paperboard the tests were conducted in 0 ° (machine direction, MD), 45 °, and 90 ° (cross direction, CD). In pretests it was determined that the specimens completely dried within 10 minutes at the specified temperature of 105 °C in a drying oven (FDL 115-230V, Binder GmbH, Germany). Afterwards, the moisture content was set by applying a specific amount of water with a spray bottle. This procedure is necessary since the maximum moisture content by hydrophilic adsorption in an air-conditioned environment is limited to about 13 % (Bedane *et al.* 2014). The required amount of water was determined by Eq. 1 DIN EN ISO 287(2009), where m_0 (g) is the dry mass, m_1 (g) is the target weight of the moistened sample, and m (%) is the pursued moisture content.

$$m = \frac{m_1 - m_0}{m_1} * 100\% \quad (1)$$

To determine the final moisture content, all specimens were weighed immediately before starting the test.

It is known that the drying of paper influences the material properties (Östlund 2005). In order to exclude this influence in the present investigations, all samples were dried before the various experiments and then moistened.

Based on the results of the conducted tensile tests, the spring back behavior was determined by loading the samples to 50 and 80 % of the maximum tensile strength. The maximum loading was set to 80 % to ensure that no specimen will break, due to the strength variations, which are a result of material inhomogeneity (Nazhad *et al.* 2000). After loading to 50 or 80 %, the load was immediately reduced at the same rate (10 mm/min) as during loading. All test parameters are summarized in Table 2.

Table 2. Test Parameters for Tensile Tests

Parameter	Variations	
Fiber orientation	0° (MD), 45°, 90° (CD)	
Moisture content	4.5 %, 10 %, 15 %, 17.5 %, 20 %, 22.5 %, 25 %	
Load before unloading	50 %, 80 % of maximum tensile strength	
Constants	Pulling/unloading velocity	10 mm/min (DIN EN ISO 1924-2, 2009)

Pneumatic Bulge Test

The depicted test rig in Fig. 5 was introduced by Post *et al.* (2011). For reasons of clarity, no attachments are depicted. In contrast to the tensile test, it allows the determination of the paperboard behavior under biaxial loads. In Fig. 5 a), the initial state, and in Fig. 5 b), the state immediately before breakage, is depicted. The load is applied by pressurized air. Since paperboard is a porous material and thus permeable to air it is separated from the pressurized air by a membrane. As explained by Post *et al.* (2011), the membrane has a small Young's Modulus compared to the paperboard to assure that influences on the results are minimized. For an improved visualization the membrane is only depicted in a detailed section (Fig. 5 a).

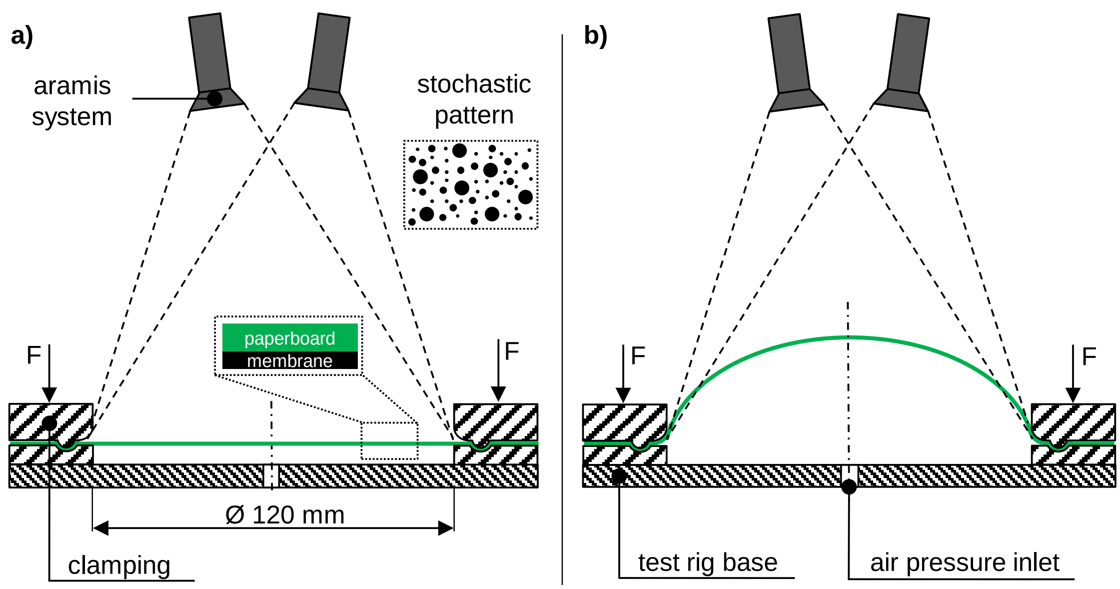

Fig. 5. Pneumatic bulge test for paperboard, a) initial state b) state before fracture

The strains are continuously determined by the optical measurement system Aramis® from GOM GmbH – Gesellschaft für Optische Messtechnik, Germany. This measurement method requires the application of a stochastic, discontinuous pattern on top of the samples. By comparing the displacement of the individual points (*cf.* Fig. 5 a), the software calculates the elongation on the basis of the initial/unloaded pattern. To determine whether the pattern influences the forming behavior, tests with and without the pattern were conducted with the result of identical pressure at break values and *vice versa*. There was no influence of the pattern on the forming behavior. The used test setup control allows investigating the forming behavior at different loading velocities and was set to 0.1 bars per second.

Huttel *et al.* (2011) and Post *et al.* (2011) determined flow curves to describe the forming limits under biaxial loads. They assumed that the material is homogenous and has a constant volume during the process. Since paperboard is comprised of a natural material, this assumption is somewhat limited (Hauptmann 2010). Therefore, no flow curves were determined for the investigations carried out. Instead, the elongation at break and the pressure at break are used as evaluation criteria as they are independent of volume. Furthermore, these parameters are less sensitive towards small irregularities like sliding of the sample out of the clamping. This makes them advantageous compared to the method used by Huttel *et al*. (2011), in which sliding is described as an impermissible process variable.

As the specimen is loaded rotationally symmetrically, the fiber orientation does not have to be considered in the test plan. The loading to determine spring back was limited to 80 % of maximum pressure-at-break value as the results of the tensile test showed a mainly elastic forming at 50 % loading. This results in the experimental plan for the bulge test shown in Table 3.

Table 3. Test Parameters for Pneumatic Bulge Test of Paperboard

Parameter	Variations	
Moisture content	4.5 %, 10 %, 20 %	
Load before unloading	80 % of maximum pressure at break value	
Constants	Loading velocity	0.1 bar/s

Test Rig for Incremental Forming

The developed test rig for the incremental forming of paperboard is depicted in Fig. 6. Compared to common test rigs for the single point incremental forming (SPIF), the test rig has a solid counter pressure assembly. The basic configuration consists of a solid plate (j), the guidance (e), and the pneumatic cylinder (g). The counter pressure assembly is used to increase the forming limits of paperboard by compressing the fiber network through the use of superimposed counter pressure, as described by Stein *et al*. (2018). Micari *et al.* (2007) described that also for the incremental forming of metal concepts, which include the application of counter pressure have been developed in order to increase shape accuracy. However, all of the described concepts support the sheet also in the flange area. Since the stiffness of paperboard is significantly lower compared to metals, the applied counter pressure will lead to unwanted bulging. Other concepts require a second drive for a counter tool and thus increase the process complexity significantly. In order to investigate the influence of paperboard support during forming, polymeric plates (j) (EPDM polymer, hereafter: EPDM-layer) can optionally be applied to the surface of the counter pressure unit. Compared to the metallic concepts, however, this support is limited to a small area around the forming zone. As this layer is only elastically formed, it can be reused.

An additional polymer layer (i) (polyethylene – PE, hereafter: PE layer) can be set on top of the paperboard to increase the contact area and to prevent grooving. This layer is first formed and then reformed to its original shape by heating under pressure in a separate process to reuse the plates.

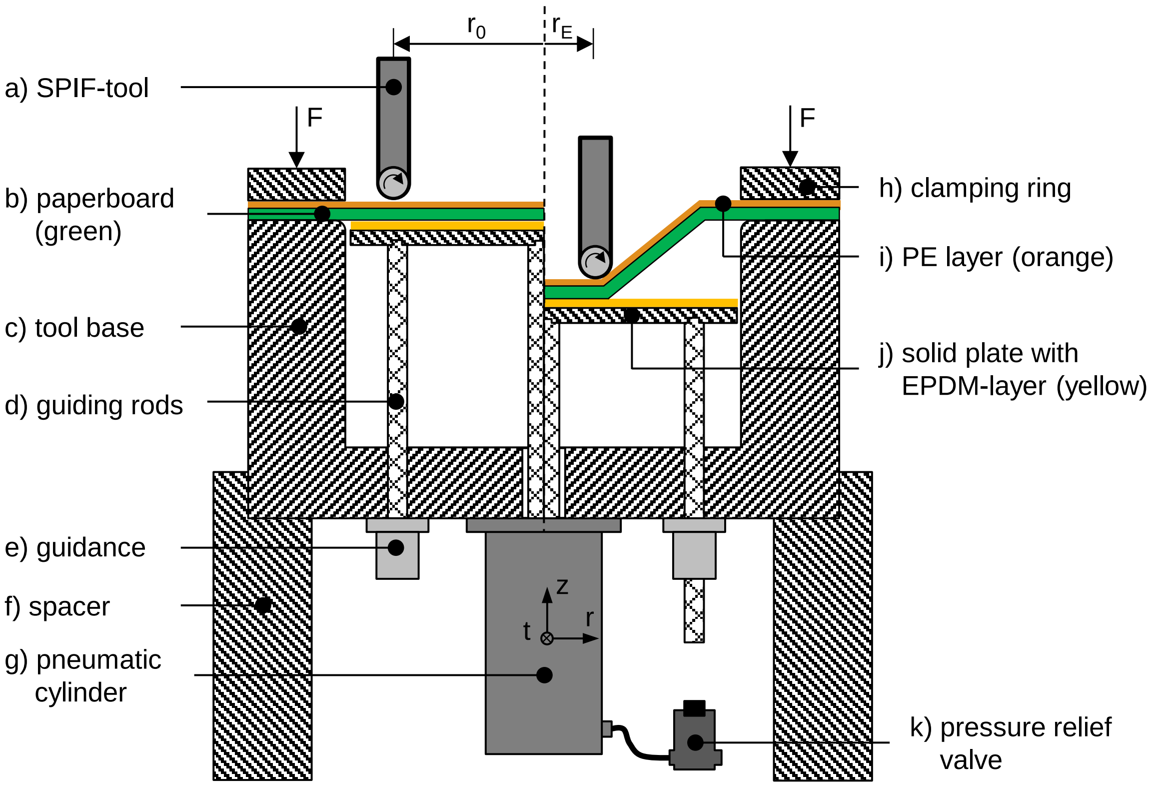

Fig. 6. Schematic test rig for the single point incremental forming of paperboard with counter pressure device, left: initial state; right: final state (not scaled)

As mentioned, the forming limit for incremental forming is usually determined by the maximum achievable flange angle. However, the flange angle is dependent on the maximum infeed in z-direction per rotation and the spring back behavior of the material. Therefore, to determine a process limit independent of the spring back, the maximum infeed in z-direction is first examined as a function of the parameters presented in Table 4. The process limit is defined as the maximum infeed in the z-direction, which can be reached without cracks in the paperboard. The maximum achievable flange angle is separately investigated by evaluation of the final part geometry. Thus, the final shape of each specimen without elastic strains is determined. For this purpose, the geometry of all parts are digitalized after the forming process with the optical measurement system ATOS® from GOM.

To reduce the influencing parameters, the infeed in radial direction is constantly set to 2.5 mm per rotation, starting at an initial radius (r_0) of 125 mm and ending at a radius (r_E) of 25 mm. Furthermore, the number of rotations is set to 40. As a result, a higher infeed value leads to a deeper cup with a steeper flange angle if spring back is not taken into account.

Compared to conventional SPIF-tools for metals, the used one (a) is not rigid, but has a rotating ball as a tip. Preliminary tests have shown that a rigid tool destroys the paperboard by shearing the top layer within the first few rotations, as a result of high friction. This failure mode is eliminated by the mounted ball. The use of lubricants to reduce friction is not suitable, as they would penetrate into the fiber network and contaminate it.

According to Groche and Huttel (2016) and Stein *et al*. (2018), the counter pressure is set to 2 and 4 N/mm². Due to the numerous elastic components in the construction, the determination of the necessary pressure (pneumatic cylinder) to achieve the required contact stresses was only approximately possible. In order to determine the real contact stresses subsequent tests were conducted. The resulting contact stresses were determined with the aid of a pressure measuring foil of the medium pressure type, mono sheet from Fujifilm, Japan.

Since the moistened samples dry during the process and thus the formability decreases, the tool velocity was set to 5000 mm/min. In order to counteract the drying of the samples, the influence of additional steam application during the process was investigated. Therefore, steam is applied through a nozzle every second rotation in front of the forming zone. All conducted process parameters are summarized in Table 4.

Table 4. Test Parameters for Incremental Forming of Paperboard

Parameter	Variations	
Moisture content	4.5 %, 10 % and 20 %	
Counter pressure	2 N/mm² and 4 N/mm²	
Thickness of EPDM layer	0, 2 mm and 6 mm	
PE layer on topside	With and without	
Steam application	With (every second rotation) and without	
Constants	Forming velocity	5000 mm/min
	Initial radius	r_0 = 125 mm
	End radius	r_E = 25 mm
	Radial infeed	2.5 mm/rotation

Additionally to the shape analysis, the forming forces were measured. In order to do so, a three axis piezo sensor (Type 9047C) from Kistler Instrumente GmbH, Germany was used. This sensor allows the measurement of the vertical, radial and tangential forces during the process. The sensor is mounted in the direct flow of force between the SPIF-tool and the chuck of the used CNC mill. The scanning frequency was set to 1200 Hz.

As it was the aim to predict the forming limits in incremental forming by standardized material characterization tests, plastic elongations were determined by the optical measurement system Argus® from GOM. The measuring principle is similar to that of Aramis®. However, in contrast to Aramis® an abrasion-resistant, deterministic pattern was applied by printing, and only one camera was needed. The plastic elongations were determined by comparing the shape of the pattern before and after the forming process.

RESULTS AND DISCUSSION – MECHANICAL TESTING

For clarification, the results of the tensile and bulge tests are described and discussed separately from the results of the investigations regarding the incremental forming. Therefore, in the following section, the results of the mechanical testing are described and discussed. For better presentation, the examinations onto tensile and bulge test are shown separately. At least five specimens were used for all parameter combinations to calculate an average value.

The section "Results and Discussion – Mechanical Testing" is followed by the section "Incremental Forming of Paperboard", which contains the results of incremental forming with a focus on process limits and shape accuracy.

Forming Behavior under Uniaxial Loads

Figure 7 depicts the elongation at break and the strain at break values dependent on the moisture content and the fiber orientation. A transversal contraction was not determined. This is further demonstration that the assumption of a constant volume during the forming processes is limited.

The elongation at break tended to a maximum at about 20 % moisture content for all fiber orientations. As already described, the general increase in elongation up to 20 % moisture content is based on weaker hydrogen bonds, which results in an easier fiber movement. The 20 % moisture content is also the value above which the influence of hydrogen bonds significantly decreases (Bos *et al.* 2006c).

As Huttel (2015) determined the maximum elongation at break at a moisture content of 15 % for a recycled paperboard, it can be concluded that the most suitable moisture content regarding high elongations at break has to be determined for each material composition individually.

In contrast to the elongations at break, the tensile strength is decreasing almost linearly with increasing moisture content. Since in CD fewer hydrogen bonds contribute to the tensile strength compared to MD, the decrease is lower. With moisture contents above 20 %, the difference is reduced to a minimum, since the hydrogen bonds no longer contribute to the cohesion of the fiber network that much.

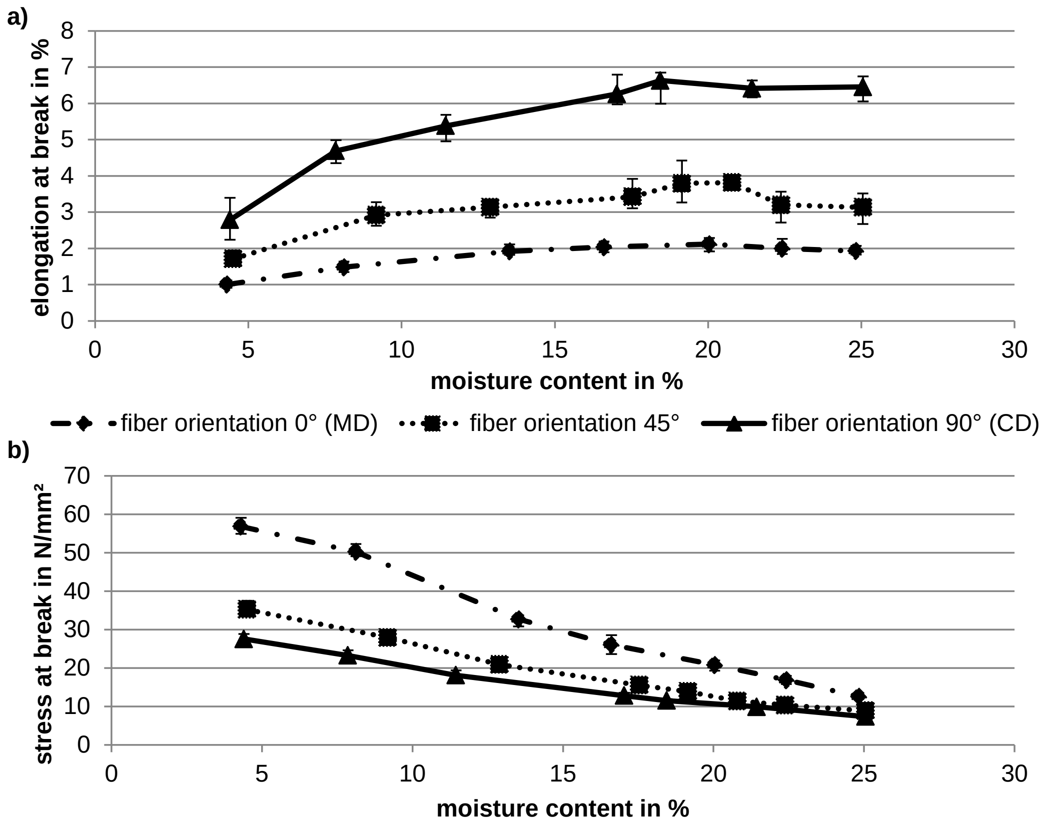

Fig. 7. a) Elongation at break and b) stress at break of fresh fiber paperboard (390 g/m²) dependent on the moisture content

Spring Back Behavior under Uniaxial Loads

Based on the presented results, the investigations regarding the spring back behavior at uniaxial loads were reduced to moisture contents of 4.5 %, (equilibrium at standard conditions), 10 % (intermediate), and 20 % (maximal elongation at break).

As depicted in Fig. 8, the spring back depends on the fiber orientation and on the moisture content. The influence of the moisture content is also explained by weakened hydrogen bonds at elevated moisture contents. Subsequently, the raising stresses between the fibers are reduced, which leads to a decreased restoring force.

The lower spring back in 45° and CD compared to MD is due to the behavior of the fiber network under load. As described in the sub-section "anisotropic forming behavior", in CD less fibers are orientated in loading direction. In consequence, fewer hydrogen bonds between the fibers are influenced, which results in a reduced restoring force. Furthermore, the distance between the fibers increases, due to the higher bearable elongations in CD with the result of fewer hydrogen bonds interacting between the fibers. The lower spring back in CD also indicates that straightening the curled fibers causes less stress in the material than the fiber elongation in MD.

For the 50 % loading, similar tendencies as above were determined. However, at 50 % the moisture content was the dominant parameter. Since the resulting elongations were low, it was assumed that almost no fiber movement occurred. As a consequence, the plastic elongations had to be based on an elongation of the highly moisture-content-dependent hydrogen bonds or a stretching of the fibers. The latter forming mechanism is assumed to be primarily limited to MD and occurring already at low loads. Thus, a low increase of + 14.7 % to 89.4 % spring back at 4.5 % moisture content compared to 80 %

loading can be explained. In contrast, spring back increased by 50.2 % in CD compared to 80 % loading. This supports the assumption that at 50 % loading the elongations in CD are too small to overcome the hydrogen bonds, which results in a high restoring force.

Due to the low absolute elongations, the quota of elastic elongations is high. Thus, the spring back values are in general higher.

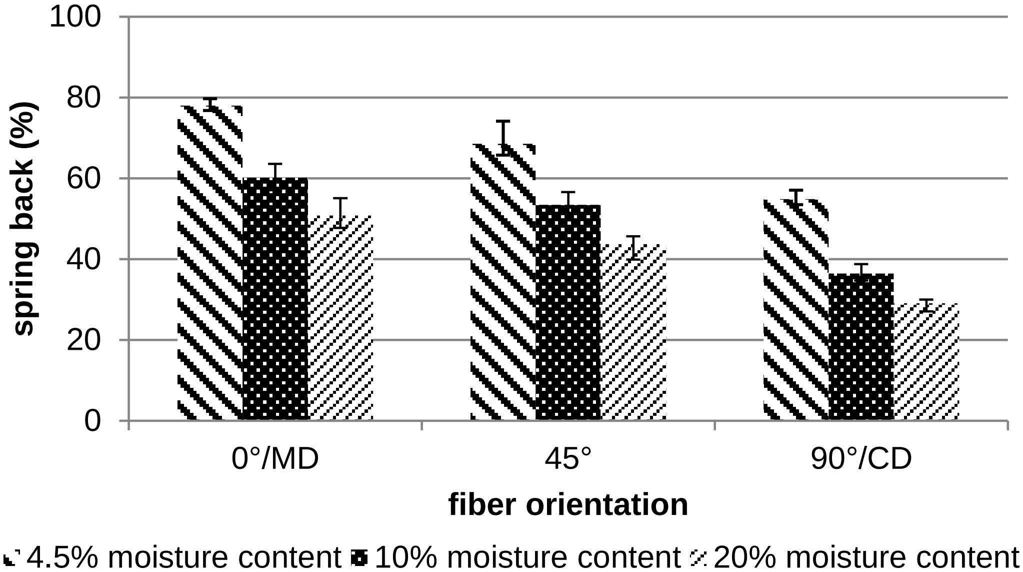

Fig. 8. Spring back dependent on the fiber orientation and the moisture content at 80 % loading of the corresponding stress at break value

Forming Behavior under Biaxial Loads

Figure 9 shows the elongations at break at 4.5 % and 20 % along a section. For this, the last image immediately before breakage is evaluated (scanning frequency was set to 5 Hz). While for the 4.5 %-samples the elongations were almost uniform, along the section at 20 % as well as at 10 % a maximum in the middle was observed. The reason for this is that there was no fiber movement near the clamping area. Consequently, an elongation can only be based on the forming mechanism “elongation”. Based on the high strength of the hydrogen bonds at low moisture contents, this is the dominant forming mechanism at 4.5 %. Consequently, a homogeneous distribution occurs along the section. In contrast, at elevated moisture contents the dominant forming mechanisms are based on a fiber movement with the result of higher elongations. As this mechanism is blocked near the clamping but not in the middle of the specimen, an uneven distribution occurs. To reduce the influence of the clamping, the elongations were only evaluated within a 15 mm radius around the center. The value 15 mm was selected because this area showed the highest strains in most of the samples. Furthermore, the average allows reducing the influence of local strain peaks, which are a result of the typically inhomogeneous material composition. For each sample the elongations at break were determined by generating three parallel sections in MD and CD (cf. Fig. 9).

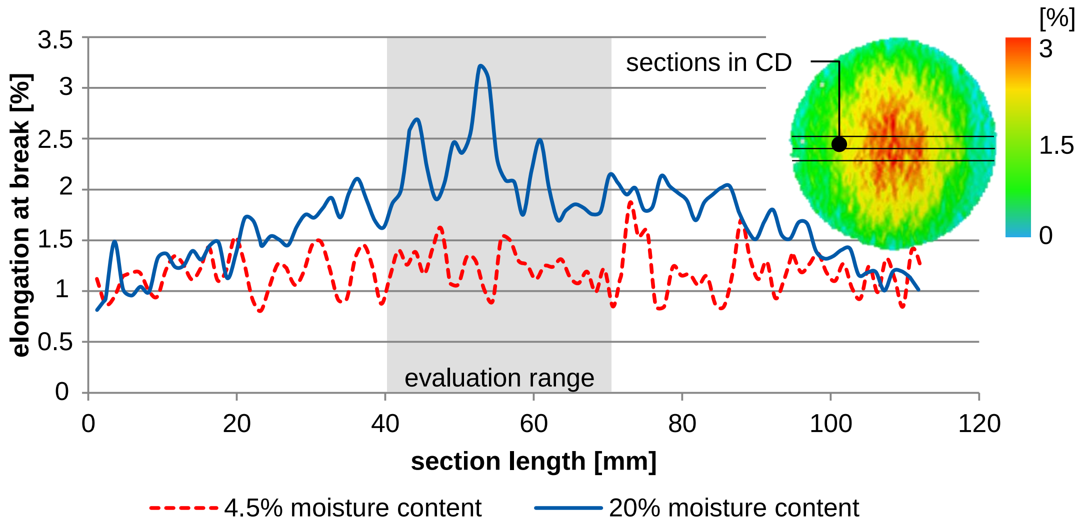

Fig. 9. Elongations at break for 4.5 and 20 % moisture content (MD) in the bulge test along a section and schematic depiction of section position on the specimen

Although the material is rotationally symmetrically loaded, the averaged elongations at break are dependent on the fiber orientation for 4.5 and 10 % moisture content (cf. Fig. 10). This occurs because of the lower forming resistance in CD than in MD, as described in the sub-section "anisotropic forming behavior". As a result, the pressurized air leads to higher elongations of the specimens in CD than in MD and thus to a deviation from an ideal circular shape. This corresponds also with the stresses at break in the tensile tests (cf. Fig. 7 b), which are always higher in MD than in CD with the same parameters.

At 20 % the elongations at break in MD and CD converged, since the fiber movement was significantly increased in both directions by the weakened hydrogen bonds. In contrast to the tensile test, however, the values were lower compared to 10 % moisture content. As can be seen in Fig. 10, the elongations at break for 20 % moisture content were reduced by 29.1 % in CD and 13.2 % in MD, compared to 10 % moisture content. The difference to the tensile test is due to the larger specimen dimensions as well as the biaxial load. Both factors lead to the fact that, in addition to the hydrogen bonds, mechanical hooking of the fibers also contributes to the fiber network strength. While hydrogen bonds allow the fiber network to be stretched, mechanical hooking can only transmit a specific force. If this force is exceeded, this bond will fail immediately. It can be assumed that the swelling of the fibers and the lower friction between the fibers caused by moisture reduce the strength of the mechanical hooking. The easing of the mechanical hooking, however, directly influences the molecular-level hydrogen bonds, since the distance between the fibers increases as a result of the loosening. As a result, the hydrogen bonds are also weakened or broken. Due to the aforementioned characteristics, the bearable elongations in the bulge test are higher at 10 % than at 20 % moisture content. The same applies to the strength of the fiber network. While the pressure at break at 10 % moisture content is 0.99 bar, it decreases to 0.40 bar at 20 %.

In the tensile test mechanical hooking has no such influence since the width of the samples is much smaller than their length. As a result, only few mechanical hooking connections are loaded with the consequence of a hydrogen bond dominated forming behavior.

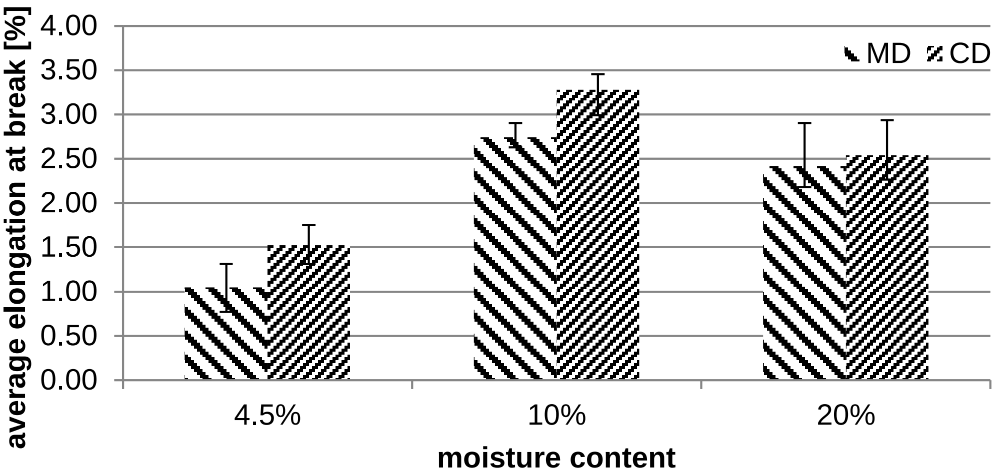

Fig. 10. Average elongation at break in MD and CD over a section of 15 mm length to both sides of the center

Huttel reported that the elongations at break for a recycled paperboard in the bulge test almost correspond to the elongations at break under uniaxial load in the 45°-fiber-orientation (Huttel 2015). For the investigated material this cannot be confirmed. In contrast to the investigations of Huttel, the used fresh fiber material showed differences regarding the elongations at break in MD and CD in the bulge test (especially at 4.5 and 10% moisture content). The main reason for these differences is that the material properties of fresh fiber paperboard commonly have higher variances between MD and CD, compared to recycled paperboard. This is due to longer fibers on the one hand and less filler material on the other hand in fresh fiber compared to recycled paperboard.

However, the ratio between the elongations at break in MD and CD (δ) in the bulge test was significantly lower compared to the tensile test (*cf.* Table 5). The reason for this is that in the bulge the fiber network is simultaneously loaded in MD and CD, which leads to homogenization. The homogenization even increases if the moisture content is further increased (20 %) and thus the hydrogen bonds are further weakened as depicted in Fig. 10 and Table 5.

Table 5. Comparison of the δ in Tensile and Bulge Test

$\delta = \varepsilon_{MD}/\varepsilon_{CD}$		
Moisture content	**Tensile test**	**Bulge test**
4.5 %	0.3571	0.6907
10 %	0.3366	0.8353
20 %	0.3281	0.9527

Spring Back Behavior under Biaxial Loads

For the spring back tests 80 % of the pressure at break is set as maximum load. This results in a maximum pressure value of 1.05 bar for 4.5 % moisture content, 0.79 bar for 10 % and 0.32 bar for 20 % moisture content.

Just as for the elongations at break, the lowest value regarding the spring back was achieved at 10 % instead of 20 %, as can be seen in Fig. 11 (cf. Fig. 8). Since the elongations at 10 % were highest, the quota of plastic strain was also highest, which results in a smaller spring back. The approach of superimposed forming mechanisms, as described in the previous section, is supported by the fact that, in contrast to the tensile tests, the spring back in MD and CD was almost identical for all moisture contents.

The reason for the higher spring back values at 20% compared to 4.5% is explained by the lower stiffness of the moistened samples. As a result, the shaped dome relaxes more. Since the dimensional stiffness in the tensile test has no influence due to the vertical clamping, this behavior is limited to the bulge test.

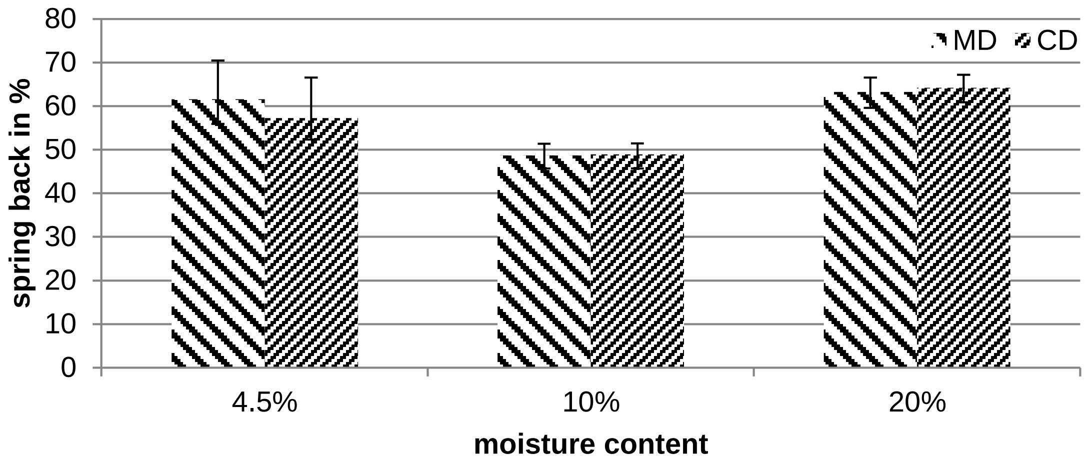

Fig. 11. Average spring back values in MD and CD after loading to 80% of pressure at break

RESULTS AND DISCUSSION – INCREMENTAL FORMING OF PAPERBOARD

The investigations concerning the incremental forming of paperboard are divided into two main sections. First, the process limits that are dependent on specific parameters are determined. However, the maximum infeed is only a single process parameter that serves as a first indication of the maximum achievable depth of the formed part (cf. section "test rig for incremental forming"). Therefore, the final geometry of the component is analyzed in the second section. Since the aim is to predict the forming behavior using standardized characterization tests, the determined influence of the various parameters is compared with the forming behavior in the characterization tests in both sections.

For reasons of clarity the nomenclature described in Table 6 is used. Due to the different polymer layers the contact normal pressure differs as the penetration depth of the SPIF-tool varies. Therefore, the counter pressure is given by the set pressure value at the pneumatic cylinder.

Table 6. Used Nomenclature

Example nomenclature: 20%_p1.2_1_6mm		
	Meaning	**Variations**
20%_	Moisture content in %	4.5, 10 and 20%; xx% includes all three designations
p1.2_	Adjusted pressure value in the cylinder in bar	p0 and p1.2
1_	With or without PE layer on topside of the paperboard	0 (without) or 1 (with)
6mm	Thickness of the EPDM layer on top of the counter pressure assembly	0 (no layer), 2 and 6 mm

In the conducted SPIF tests the moisture content of the samples with an initial moisture content of 20 % was reduced by only 2 % since no tool parts were heated. As a consequence, the additional steam application easily leads to moisture contents above 10 % (bulge test) or 20 % (tensile test) and thus reduces the formability, as shown by the conducted material characterization tests. Even in the tests with an initial moisture content of 4.5 % no advantage is determined. Since none of the tool parts are heated, the applied steam condenses immediately, which leads to puddles on the paperboard. The high amount of water causes a significant softening and finally a decomposition of the fiber network due to the mechanical stress. Thus no further tests were conducted with steam.

Process Limits

Figure 12 depicts the maximum infeed for incrementally formed parts at different conditions.

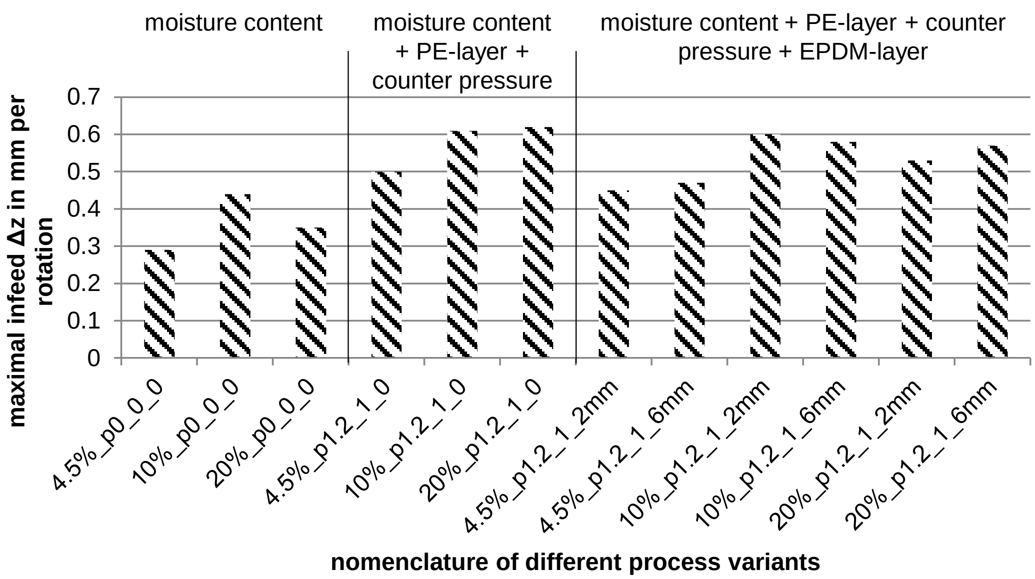

Fig. 12. Maximal infeed (Δz) per rotation dependent on different process parameters

As assumed, known optimization parameters, like elevated moisture content and a counter pressure, in general increase the maximum infeed.

Contrary to the initial assumption, an EPDM-layer mounted to the counter pressure assembly (xx%_p1.2_1_2mm and _6mm) does not further increase the maximum infeed compared to the test setup with counter pressure only (xx%_p1.2_1_0). Rather, the additional layer even slightly reduces the maximum infeed. Investigations regarding the final thickness of the formed specimens show that the compression is negligibly small when using the EPDM-layer. This compression, however, is required to increase the forming limits of paperboard as presented by Stein *et al*. (2018). Without the EPDM-layer but with a PE-layer a compression from 0.52 to 0.45 mm (-13.46 %) for dry samples and from 0.56 to 0.44 mm (-21.24 %) for moistened samples was determined, when superimposing a counter pressure. It is assumed, that due to the EPDM-layer the forming area is increased and thus the resulting contact normal pressure is too low to compress the paperboard. This was confirmed by the tests with a pressure measuring foil. It is determined that at 4.5%_p1.2_1_0 the contact normal pressure is 6.78 N/mm². At 4.5%_p1.2_1_6 mm, the contact normal pressure was only 1.24 N/mm² and thus obviously too small to sufficiently compress the paperboard. The contact normal pressures of all other tests were within this range with highest values at 4.5%. This behavior can be explained as follows. Moistening causes the paperboard to swell and the pressure resistance is reduced. At the same time, however, the counter pressure in the pneumatic cylinder is constantly set to 1.2 bar for all tests. Since the PE-layer is used in all tests when applying a counter pressure, the forming area is not limited to the SPIF-tool diameter only. As a result, the constant counter force acts on a larger surface, resulting in smaller compression values for moistened samples.

As already mentioned, the PE layer is always used when applying a counter pressure. The reason for this is that the penetration of the SPIF-tool into the paperboard by the counter pressure leads to grooves when the PE layer is not used.

Process limits compared to the mechanical characterization tests

Without a counter pressure, the maximum infeed followed the forming behavior in the bulge test with the highest infeed at 10% (10%_p0_0_0). The same was determined when using an EPDM-layer on top of the counter pressure assembly. In case of only applying a counter pressure (xx%_p1.2_1_0), the maximum infeed followed the behavior within the tensile tests with the highest infeed at 20%. This was due to the direct contact of the paperboard with the solid counter pressure assembly (aluminum). The contact area and thus also the forming area was strongly localized (Fig. 13b).

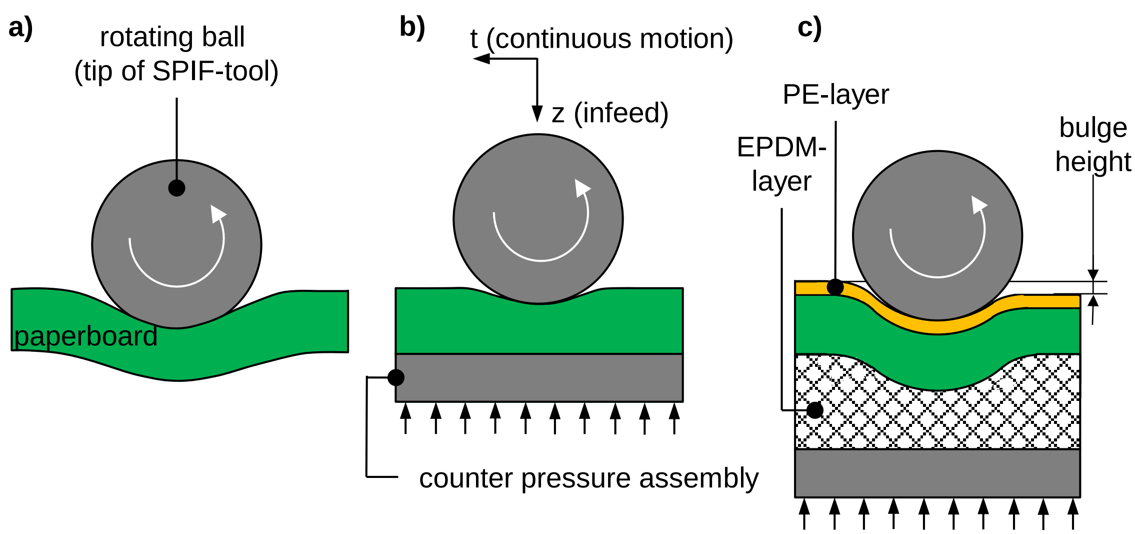

Fig. 13. The different forming conditions dependent on the set up, no scaling

As a result, the interaction of the fibers was reduced, as only a few were loaded simultaneously. In contrast, at xx%_p0_0_0 the paperboard surrounded the SPIF-tool during the forming process with the result of an interacting of the fibers as in the bulge test (Fig. 13a). The same phenomenon occurred when using the EPDM-layer (Fig. 13c). Due to the counter pressure and the forming force, the polymer was compressed and thus a cavity emerged in which the paperboard was formed. As a consequence of the cavity on the one hand side the paperboard also encircled the SPIF-tool. On the other hand, the compression leads to a restoring force applied by the EPDM-layer, which additionally pushes the paperboard against the SPIF-tool.

The maximum elongations in tensile-, bulge-test, and SPIF (4.5%/10%_p0_0_0) are depicted at 4.5% and 10% moisture content in Fig. 14. However, due to the counter pressure assembly, no inline measurement of elongations was possible. Thus, in SPIF only plastic elongations were determined. As a consequence, the depicted elongations for tensile and bulge test in Fig. 14 are also the plastic part, determined after loading to 80 % of strength at break and a subsequent unloading. It is obvious that the elongations in SPIF were significantly higher (between 1.30- and 4.52-times) than expected from the material characterization tests. The difference was approximately equal to the spring back values in the characterization tests. Nevertheless, spring back also occurred in SPIF (*cf.* subsection “shape accuracy”). As a consequence, it can be concluded that the bearable elongations during the SPIF process were higher compared to the characterization tests. This meets the state of the art for which higher elongations can be endured in SPIF compared to other forming processes due to the localized forming. This behavior can be explained on the one hand by compression of the fiber network even if no counter pressure is applied, due to the forming resistance of the sheets. For 4.5 % a reduction from 0.52 mm to 0.50 mm is determined. For 10 % a reduction from 0.54 to 0.50 mm is observed. On the other hand the localized and repetitive forming (Fig. 19 in section “vertical spring back”) leads to an improved forming behavior.

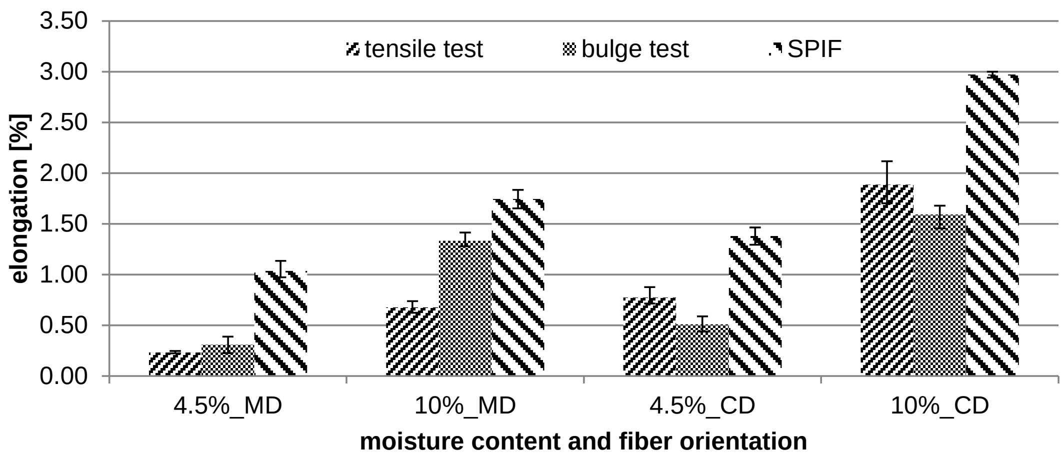

Fig. 14. Comparison of the plastic elongations in tensile-, bulge test and SPIF

Figure 15 shows the elongations in SPIF of all parameter combinations. The highest plastic elongations occurred at 10 %. This behavior is similar to the bulge test. This data also confirmed that the difference between MD and CD was reduced at 20 %. Furthermore, the elongations were increased for all moisture contents by applying a counter pressure, which is explained by compression of the fiber network (Stein *et al*. 2018). However, the compression is dependent on the set parameters.

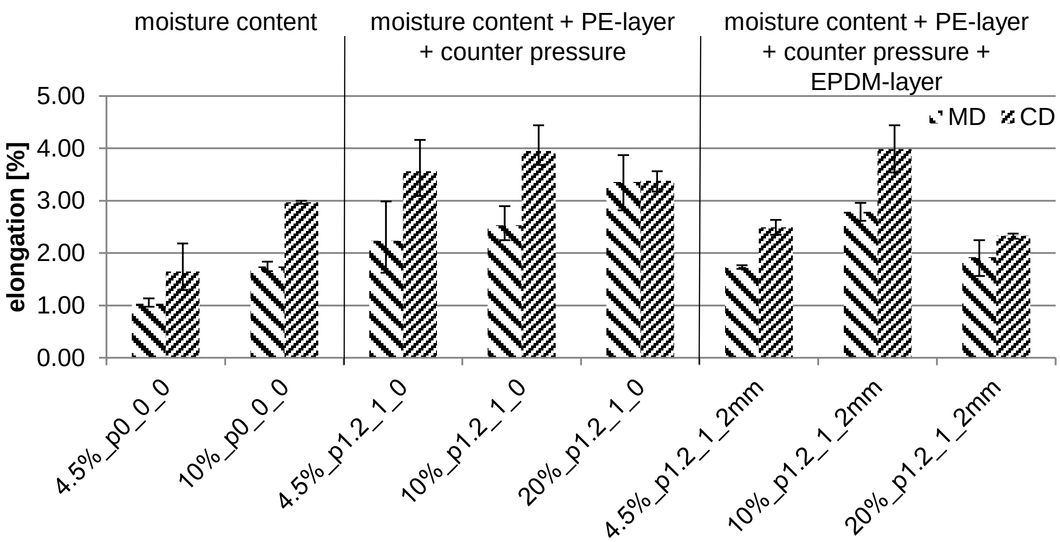

Fig. 15. Plastic elongations in SPIF at different parameter combinations

Influence of tangential forces on to the achievable forming limits

Based on the depicted forming conditions in Fig. 13, it is expected that an increase of the counter pressure will lead to an increased compression of the fiber network and thus to extended forming limits. However, this was not the case. Increasing the counter pressure without any polymer layer tangential forces will limit the forming, as they cause twisting. This behavior is also known for metals (Neto *et al.* 2015). The tangential forces are based on a deeper penetration of the SPIF-tool into the paperboard as a result of the higher counter pressure values. Due to the continuous moving of the SPIF-tool this leads to an increased bulge in front of the forming tool (*cf.* Fig. 13 c), which causes tangential forces and in consequence a twisting of the samples.

However, increased tangential forces do not always lead to twisting. In Fig. 16 a) the tangential forces are depicted for 0.5 and 1.2 bar cylinder pressure with the use of the PE-layer between the SPIF-tool and the paperboard. As expected, the tangential forces increased with high counter pressure. In contrast to the forming without the PE-layer no twisting occurred. The reason for this is, on the one hand, that the tangential force was increased primarily by a deeper penetration of the SPIF-tool into the PE-layer. The penetration into the paperboard was reduced by the increased forming surface and as a consequence, the lower contact pressure by the use of the PE-layer as depicted before. On the other hand, friction occurs between the paperboard and the PE-layer, which reduces twisting as the resulting friction force is counteracting the tangential force. Thus, by the use of the PE-layer the introduced tangential stresses onto the paperboard are reduced and the failure mode switches from twisting to a fiber network breakage.

Vertical forces at incremental forming of paperboard

It is obvious, that the vertical forces (z-direction) rose with the increase of the counter pressure (cf. Fig. 16 a). The compression of the PE-layer and, if used, the EPDM-layer led to a reduced force in z-direction at the first two rotations, as can be seen in evidence for 1.2 bar. This is due to the fact, that the counter pressure assembly has a limit stop at the level of the clamping. Since the starting point ($z = 0$) is set on top of the PE-layer the first two rotations are required to compress the PE-layer and possibly the EPDM-layer.

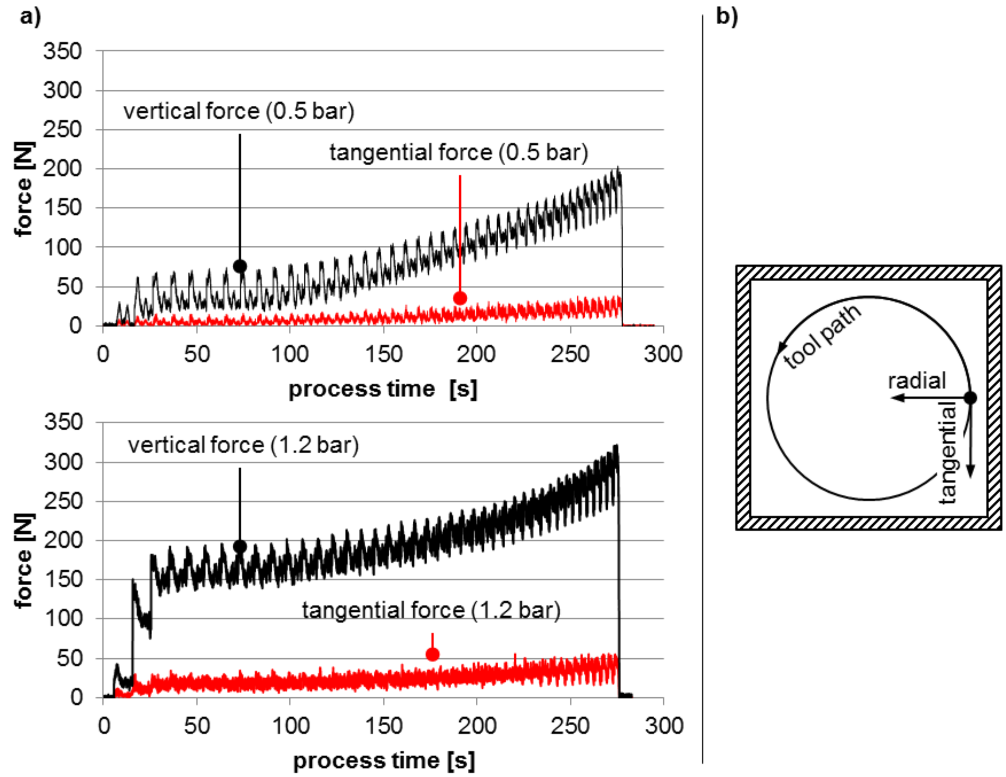

Fig. 16. a) forming forces at SPIF of paperboard with 0.5 bar (top) and 1.2 bar (bottom) cylinder pressure with PE-layer at 4.5 % moisture content; b) horizontal force components at SPIF

Further features of the force-time curve

For the sake of completeness the force over process time curve will be explained in greater detail. As can be seen in Fig 16 a), the forces increased during the process. This is explained by the growing contact area between the SPIF-tool and the paperboard as well as the PE-layer due to the developing conical shape. Furthermore, the forming resistance and the elastic restoring forces of the materials increase, which leads to higher forming forces. Tests without any layer (SPIF-tool + counter pressure only) show an almost constant progression. The oscillation of the curves is generally explained by the fact that the pressure has to be adapted first at every infeed by the pressure relief valve as the pressure increases due to the pressing of the piston rod into the cylinder. The higher frequency at the end of the process is explained by the reduced diameter.

Shape Accuracy

The above described process limits are only based on the process parameters and thus do not take into account spring back. In order to determine the best parameter combination with regard to a maximum cup height and a steep flange angle, the shape of the final part has to be taken into account in comparison to the process parameters.

Because the specimens are fixed by the clamping ring (part h in Fig. 6), the most common shape inaccuracy of paperboard forming, namely wrinkles, do not occur (Hauptmann *et al*. 2016b).

As spring back is a characteristic material behavior, it also occurs during incremental forming and thus has to be investigated. Since the specimens were digitalized immediately after the forming process, it is assumed that shrinkage does not influence the results. However, there is no evaluation of samples at 20%_p0_0_0 possible. The reason for this is that this parameter combination releases the residual stresses that arise in the manufacturing process. In consequence, waves occur which are always parallel to MD and thus the specimen could not be evaluated. The orientation of the waves is explained by the higher strength in MD compared to the one in CD as well as the machine-direction-orientated, different drying conditions. For 10 % moistened samples (10%_p0_0_0) also a small waviness was determined, but was smooth enough to evaluate its shape. In tests with a superimposed counter pressure (*e.g.* 20%_p1.2_1_0) no waviness is observed.

As depicted in Fig. 17 a), the final shape is evaluated by sections in MD and CD. To determine the spring back behavior, the tool path is compared with the final shape of the parts after releasing any force and clamping. As can be seen, two kinds of spring back occurred. On the one hand, the bottom springs back in vertical direction (vertical spring back). On the other hand, the flanges differ from the tool path (spring back of the flange angle α). Additionally, a shape deviation in the bottom and transition area occurs, as can be seen in Fig. 17 a). For reasons of clarity, the influence of the investigated process parameters onto the various shape inaccuracies is afterwards described separately.

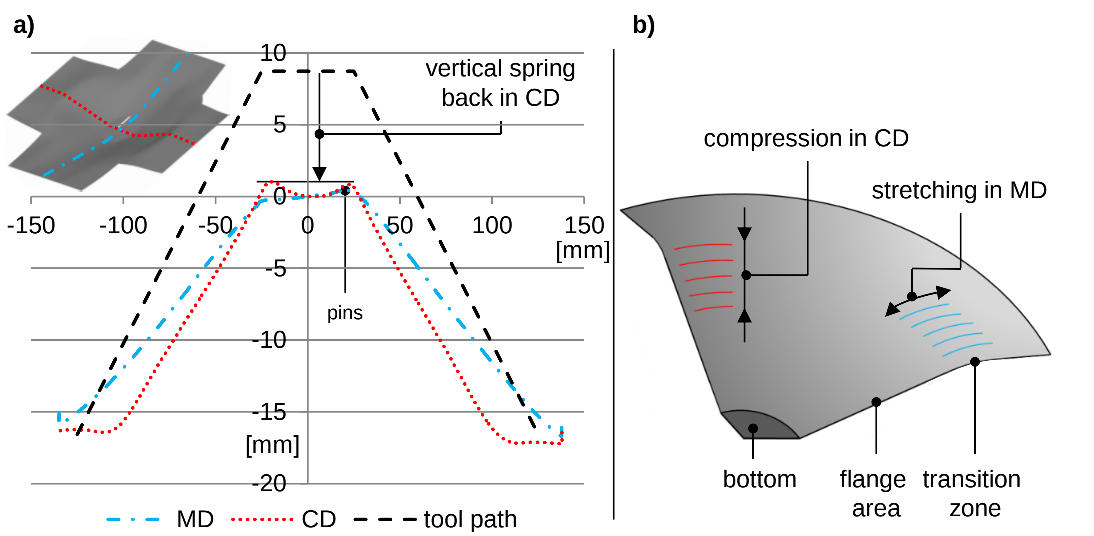

Fig. 17. a) Representative sections in MD and CD of a single point incrementally formed part; b) Schematic section of the conical shape with depicted forming behavior of the fibers dependent on their preferred orientation

Vertical spring back

The spring back values depicted in Fig. 18 refer to the depth of the tool path. A spring back of 50 % correspondingly means that the final component is only half as deep. The measurement was conducted immediately after the forming process. However, disassembly, transportation to the measurement system, and preparation for measurement required about five minutes. The difference in the vertical spring back between MD and CD is based on the fiber-orientation-dependent forming behavior. While the fibers in MD get stretched like illustrated in Fig. 17 b), in CD the load, acting perpendicularly to the fiber orientation, primarily leads to a compression of the voids between the fibers, as has already been determined by Stein *et al*. (2017). This behavior leads to a smooth radius in MD and a sharp molding, almost identical with the diameter of the SPIF-tool (15.88 mm), in CD (cf. Fig. 17 a). In consequence, in CD two "pins" occur which quantitatively reduce the spring back in vertical direction.

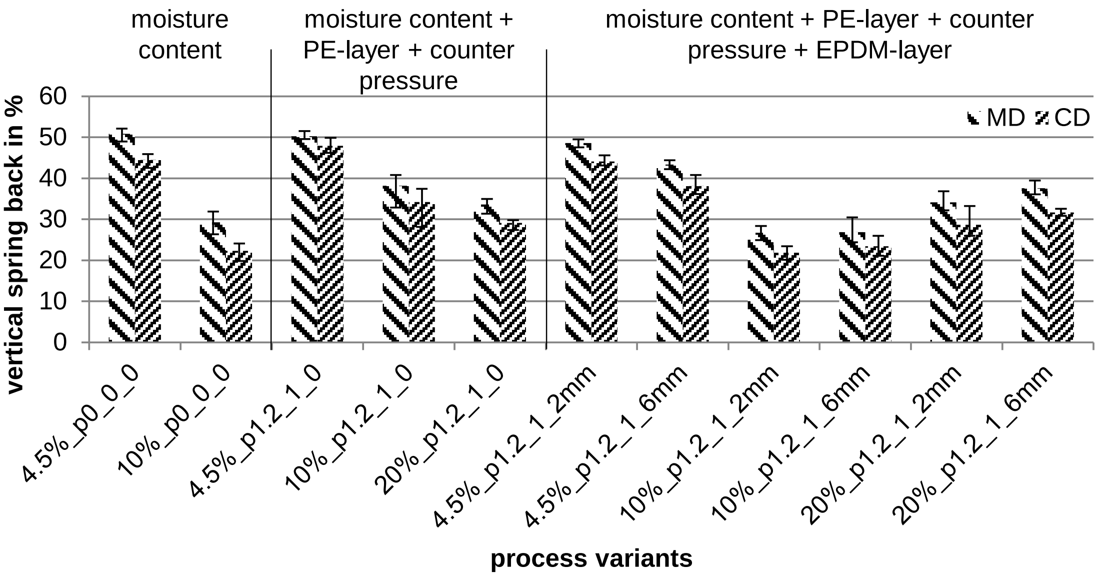

Fig. 18. Vertical spring back of incremental formed parts at different process parameters

Due to weakened hydrogen bonds, the spring back in general decreased with increased moisture content. For the parameter sets xx%_p1.2_1_0 the behavior is similar to the one with uniaxial loads. However, when additionally an EPDM-layer is used, the spring back behavior was similar to that of the bulge test with a minimum spring back at 10% moisture content. As already described in the section "process limits compared to the mechanical characterization tests", the forming is more localized if an EPDM-layer is not used on the upper side of the counter pressure assembly and therefore the forming behavior with respect to the influence of the moisture content corresponds more closely to that of the tensile tests.

Comparing the vertical spring back values with the use of counter pressure and EPDM-layer with those of the bulge test yields that, in contrast to the bulge test, spring back was smaller at 20% moisture content (20%_p1.2_1_2mm or _6mm) than at 4.5% (4.5%_p1.2_1_2mm or _6mm). As mentioned, the weight of the moistened samples influences the spring back in the bulge test. However, in the conducted incremental forming tests the vertical forming direction (z-direction) is identical to gravity. As a result, the sample weight does not reduce the component depth, nor does it increase it, as the counter pressure assembly prevents this.

In general, spring back values were lower when using an EPDM-layer on topside of the counter pressure assembly with the smallest spring back of all tests at 10%_p1.2_1_2mm. Thus, the EPDM-layer interacts with the paperboard, which results in a reduced spring back. This behavior can be explained by the increased forming area, which is a result of the use of the EPDM-layer and the counter pressure as already described in section "process limits". Due to this, the forming time is enlarged and thus the fibers have more time to restore (*cf.* section "time and temperature for increased shape accuracy"). Since the forming area is radially symmetrically enlarged around the SPIF-tool, on the one hand the forming time is enlarged within one circulation. On the other hand, the same area is already formed during the previous rotation and is formed again during the subsequent circulation (Fig. 19).

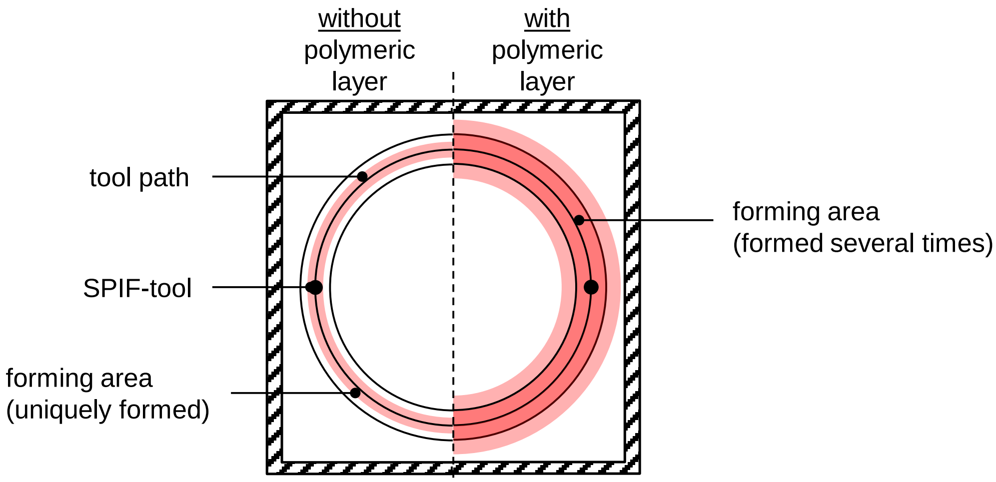

Fig. 19. Schematic depiction of the forming area, dependent on the use of an EPDM-layer

Shape inaccuracies in the transition zone

Opposite to the bottom area a significant difference regarding the final diameter occurred in the transition zone (Fig. 17 a). As described in the previous section, this was partly due to the different spring back behavior in MD and CD and due to the fibers interacting within the network. Additionally, the different forming mechanisms in MD and CD were responsible for the deviations. In MD, the fibers were loaded parallel to their orientation. Due to the hydrogen bonds, the local forming was mainly transferred in the longitudinal direction of the fiber, thus expanding the forming area. In contrast, in CD the fibers were loaded perpendicularly to their orientation with the result of a sharply formed transition area.

Spring back of the flange angle

In Fig. 20 the spring back values of the flange angle for different parameters are depicted. At first glance, some negative values in CD can be seen. This means that the final flange angle was steeper than the angle of the tool path. It is obvious that this situation predominately occurred at 4.5 % moisture content. The reason for this can be explained as follows. It is known that the spring back in MD is higher than in CD, especially at low moisture content. Additionally, the strength of the fiber network and as a consequence the fiber network interaction is the highest at low moisture contents. Thus, the spring back of the flanges in MD influences the spring back in CD by reducing the diameter primarily in the transition area (lower dimensional stiffness) with the result of a steeper flange angle compared to the tool path. Since the material behavior is homogenized (reduced interaction) at higher moisture contents no negative values occur.

Furthermore, a high difference between MD and CD occurred except for 10%_p1.2_1_2mm and _6mm. The reason for the difference is based on the diverse forming and spring back behavior in the transition zone as described the previous section.

At 10%_p1.2_1_2mm and _6mm the spring back of the flange angle in MD and CD was almost identical, which leads to almost rotationally symmetric final shapes. Additionally, for these parameters the values in MD were the smallest. As without an EPDM-layer a high difference between MD and CD is determined (10%_p1.2_1_0), this behavior must be based on support by the EPDM-layer. However, it appears that this support requires a certain degree of fiber network stiffness, as a difference between MD and CD occurs at 20 % moisture content.

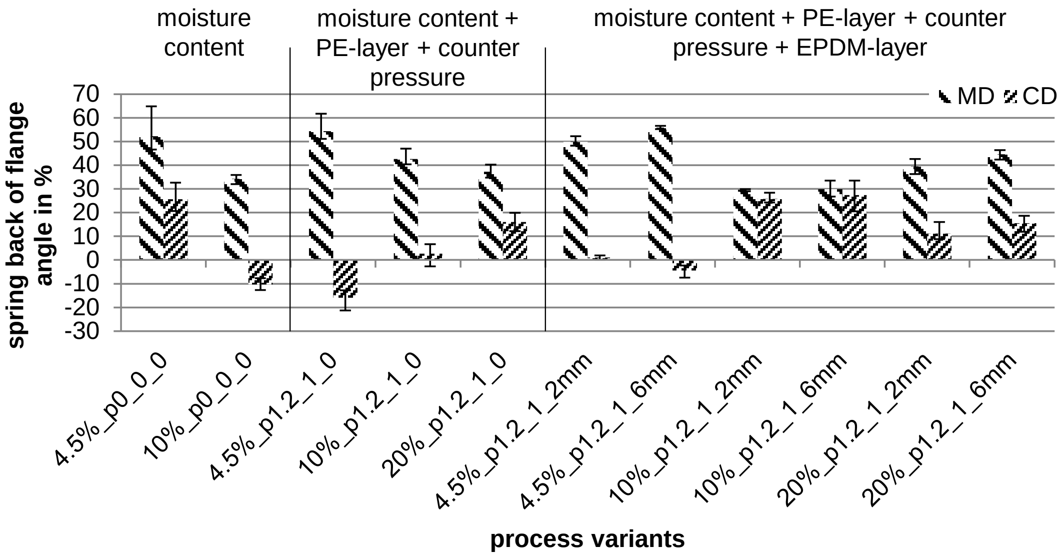

Fig. 20. Spring back towards the tool path in MD and CD dependent on different parameters

Optimized Process Parameters for SPIF of Paperboard

Figure 21 depicts the final cup height (vertical distance from the bottom to the clamping plane).

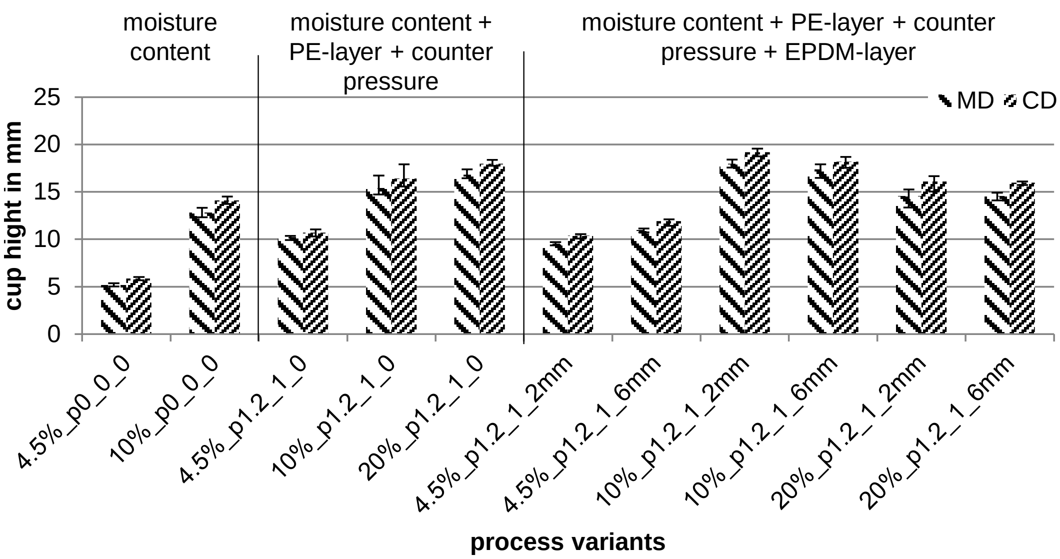

Fig. 21. Resulting cup height of incrementally formed parts at different parameters

Comparing the cup height with the maximum infeed in Fig. 12 it becomes obvious that the maximum infeed was not sufficient to predict the best parameter combination with regard to the deepest cup. While the infeed is maximal at 10 and 20% and a superimposed counter pressure only (10%/20%_p1.2_1_0), the cup height was maximal at 10% with an applied counter pressure and a thin EPDM-layer (10%_p1.2_1_2mm). This result is explained by the lower vertical spring back when using an EPDM-layer on the topside of the counter pressure assembly. With the optimized parameter combination (10%_p1.2_1_2mm), an increase of the cup height of 347% in MD and 328% in CD compared to 4.5%_p0_0_0 was achieved.

Comparing the final cup height with the conducted material characterization tests, a good accordance with the material behavior in the bulge test (Fig. 10 and 11) was observed when using an EPDM-layer. Thus it can be concluded that the bulge test is the expedient characterization method to determine the best moisture content to achieve a deep cup. This procedure is required, as it was found that the optimized moisture content is dependent on the material composition.

In Fig. 22 the final flange angle is depicted. It can be seen that the flange angle for the most parts differed significantly between MD and CD. Only at 10%_p1.2_1_2mm and _6mm an almost uniform flange angle was observed. As this parameter combination corresponds with the one for the maximum cup height, it can be concluded that the incremental forming of the investigated fresh fiber paperboard should be conducted at a moisture content of 10 % with a superimposed counter pressure and an EPDM-layer on topside of the counter pressure assembly.

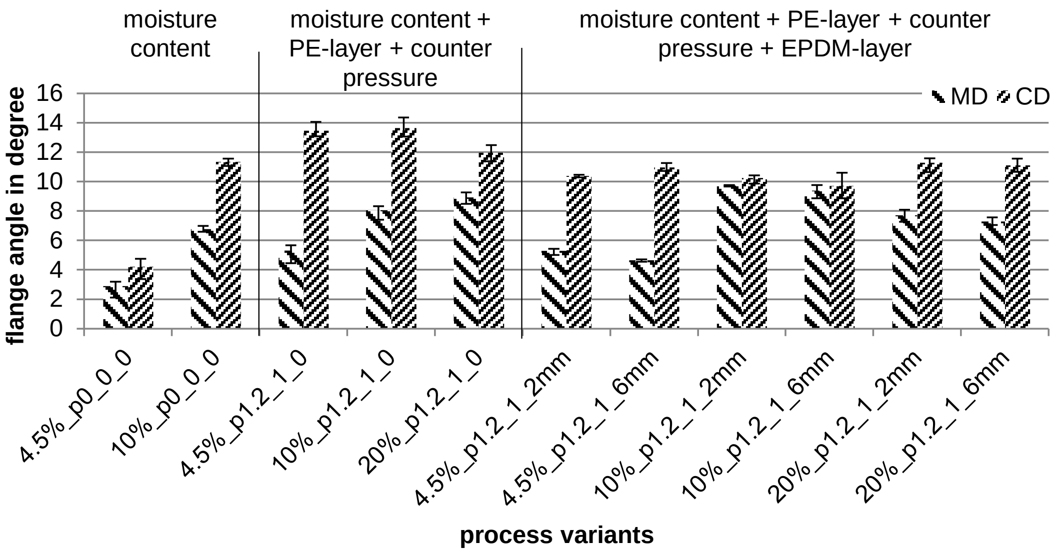

Fig. 22. Resulting flange angle of incrementally formed parts at different parameters

Outlook

To further improve the shape of incrementally formed parts, a pre-loading at the beginning of the process (transition zone) will be investigated. The aim is to immediately achieve a plastic deformation in the transition zone, as currently the forming in the transition zone is almost purely elastic. In addition, a heater will be added to the counter pressure assembly to improve the material behavior towards better formability as described in the literature and to prevent condensation of steam. This should enable the advantages of a steam application during the incremental forming of paperboard as determined by Franke *et al.* (2018).

In addition, the influence of a lower grammage as well as the paper composition will be considered in future investigations in order to examine the transferability of the findings.

Furthermore, the incremental forming of paper-based sandwich panels consisting of two thin aluminum face-sheets and a paperboard core (*e.g.* for facade applications) will be investigated. First tests showed that these panels have a better insulation than conventional (polymer-based) panels. In addition, the thin aluminum layers serve as protection against external influences such as water and insect infestation.

CONCLUSIONS

1. The ideal moisture content in order to achieve the maximum elongations at break is dependent on the material composition.
2. The maximum elongation at break does not show a linear relation to the moisture content.
3. The different forming mechanisms in MD and CD lead to significant differences in fiber-orientation-dependent spring back values with higher values in MD.
4. The differences of the material's properties between MD and CD in the bulge test are significantly lower than in the tensile test. This is explained by the interaction of the fiber network, which leads to a homogenization.
5. Due to the interaction of the fiber network at biaxial loads, the optimal moisture content to achieve a high elongation at break as well as a small spring back values switches from 20 % in the tensile test to 10 % in the bulge test.
6. In both tensile and bulge tests, the bearable elongations are lower than in SPIF.
7. A reusable counter pressure assembly is introduced and is proved to increase the forming limits of paperboard during incremental forming.
8. A PE layer between the SPIF-tool and the paperboard is useful to avoid grooves and twisting. Since PE is a thermoplastic material it can be easily recycled in a post process to increase sustainability.
9. The forming behavior at incremental forming is primarily similar to the bulge test. When using the counter pressure assembly without an EPDM-layer, the forming behavior known from the tensile test dominates as a result of the localized deformation zone.
10. The highest cup height and lowest spring back is achieved at a moisture content of 10 % with a superimposed counter pressure of about 1.7 N/mm² (resulting from 1.2 bar in the pneumatic cylinder) and a 2 mm EPDM-layer on top of the counter pressure assembly.
11. The maximum flange angles that can be achieved are significantly lower compared to most metals.
12. Because the forming behavior for the optimized parameter combination is similar to the bulge test, the optimal moisture content can be determined with this characterization test.

ACKNOWLEDGMENTS

The results presented were developed as part of the LOEWE priority program "Building with Paperboard", financed by the State of Hesse (Germany). Further thanks go to StoraEnso for providing test material. The authors also thank the German Research Foundation and the Open Access Publishing Fund of the Technische Universität Darmstadt for their support.

REFERENCES CITED

Allaoui, S., Aboura, Z., and Benzeggagh, M. L. (2009). "Phenomena governing uni-axial tensile behavior of paperboard and corrugated cardboard," *Composite Structures* 87, 80-92. DOI: 10.1016/j.compstruct.2008.01.001

Bambach, M. (2007). *Process Strategies and Modelling Approaches for Asymmetric Incremental Sheet Forming*, Ph.D. Dissertation, Rheinisch-Westfälische Technische Hochschule Aachen, Aachen, Germany.

Bedane, A. H., Xiao, H., and Eić, M. (2014). "Water vapor adsorption equilibria and mass transport in unmodified and modified cellulose fiber-based materials," *Adsorption* 20(7), 863-874. DOI: 10.1007/s10450-014-9628-6

Behera, K. B., de Sousa, R. A., Ingarao, G., and Oleksik, V. (2017). "Single point incremental forming: An assessment of the progress and technology trends from 2005 to 2015," *Journal of Manufacturing Processes* 27, 37-62. DOI: 10.1016/j.jmapro.2017.03.014

Bos, J. H., Veenstra, P., Verhoeven, H., and Vos, P. D. (2006a). "Faserstoffe für Papier und Karton," in: *Das Papierbuch – Handbuch der Papierherstellung,* 2 Auflage, Houten, Netherlands. ISBN: 978-90-01-40258-7

Bos, J. H., Veenstra, P., Verhoeven, H., and Vos, P. D. (2006b). "Blattbildung," in: *Das Papierbuch – Handbuch der Papierherstellung*, 2. Auflage, Houten, Netherlands. ISBN: 978-90-01-40258-7

Bos, J. H., Veenstra, P., Verhoeven, H., and Vos, P. D. (2006c). "Trocknung von Papier und Karton," in: *Das Papierbuch – Handbuch der Papierherstellung,* 2 Auflage, Houten, Netherlands. ISBN: 978-90-01-40258-7

Datasheet Trayforma (2018). "Trayforma™ Bio," (https://www.storaenso.com/-/media/Documents/Download-center/Documents/Product-specifications/Paperboard-materials/Trayforma-Bio-35-en.ashx), accessed 29 September 2018.

DIN 50125 (2016). "Testing of metallic materials – Tensile test pieces," DIN Deutsches Institut für Normung e.V., Beuth Verlag GmbH, Berlin, Germany.

DIN EN ISO 1924-2 (2009). "Paper and board – Determination of tensile properties – Part 2: Constant rate of elongation method (20mm/min)," DIN Deutsches Institut für Normung e.V., Beuth Verlag GmbH, Berlin, Germany.

DIN EN ISO 287 (2009). "Paper and board – Determination of moisture content of a lot – Oven-drying method," DIN Deutsches Institut für Normung e.V., Beuth Verlag GmbH, Berlin, Germany.

Franke, W., Stein, P., Dörsam, S., and Groche, P. (2018). "Formability of paperboard during deep-drawing with local steam application," in: *AIP Conference Proceedings of the ESAFORM conference*, Palermo, Italy, 1960, 100008. DOI: 10.1063/1.5034948

Golzar, M., and Ghaderi, A. (2009). "Effect of temperature on the spring back of cellulose-based sheet in hot pressing" *International Journal of Advanced Manufacturing Technology* 42, 633-642. DOI: 10.1007/s00170-008-1626-y

Groche, P., and Huttel, D. (2016). "Paperboard forming – Specifics compared to sheet metal forming," *BioResources* 11(1), 1855-1867. DOI: 10.15376/biores.11.1.1855-1867

Haslach, H. W. (2000). "The moisture and rate-dependent mechanical properties of paper: A review," *Mechanics of Time-Dependent Materials* 4 (3), 169-210. DOI: 10.1023/A:1009833415827

Hauptmann, M. (2010). *Die gezielte Prozessführung und Möglichkeiten zur*

Prozessüberwachung beim mehrdimensionalen Umformen von Karton durch Ziehen, Ph.D. Dissertation, Technische Universität Dresden, Dresden, Germany.

Hauptmann, M., and Majschak, J.-P. (2011). "New quality level of packaging components from paperboard through technology improvement in 3D forming," *Packaging Technology and Science* 24, 419-432. DOI: 10.1002/pts.941

Hauptmann, M., Wallmeier, M., Erhard, K., Zelm, R., and Majschak, J.-P. (2015). "The role of material composition, fiber properties and deformation mechanisms in the deep drawing of paperboard," *Cellulose* 22, 3377-3395. DOI: 10.1007/s10570-015-0732-x

Hauptmann, M., Weyhe, J., and Majschak, J.-P. (2016a). "Optimisation of deep drawn paperboard structures by adaption of the blank holder force trajectory," *Journal of Material Processing Technology* 232, 142-152. DOI: 10.1016/j.jmatprotec.2016.02.007

Hauptmann, M., Kaulfürst, S., and Majschak, J.-P. (2016b). "Advances on geometrical limits in the deep drawing process of paperboard," *BioResources* 11(4), 10042-10056. DOI: 10.15376/biores.11.4.10042-10056

Havimo, M., Jalomäki, J., Granström, M., Rissanen, A., Iivanainen, T., Kemmel, M., Heikkilä, M., Sipi, M., and Kilpeläinen, I. (2011). "Mechanical strength and water resistance of paperboard coated with long chain cellulose esters," *Packaging Technology and Science* 24, 249-258. DOI: 10.1002/pts.932

Hirt, G., Ames, J., Bambach, M., and Kopp, R. (2004). "Forming strategies and process modelling for CNC incremental sheet forming," *CIRP Annals* 53 (1), 203-206. DOI: 10.1016/S0007-8506(07)60679-9

Huttel, D., Post, P.-P., Schabel, S., and Groche, P. (2011). "The stress strain behaviour of paperboard in tensile and bulge tests," in: *Proceedings to the 10th International Conference on Technology of Plasticity*, Aachen, Germany.

Huttel, D., and Groche, P. (2014). "New hydroforming concepts for sustainable fiber material (paperboard)," *International Conference New Developments in Hydroforming*, Fellbach, Germany, pp. 127-141.

Huttel, D. (2015). *Wirkmedienbasiertes Umformen von Papier*, Ph.D. Dissertation, Technische Universität Darmstadt, Darmstadt, Germany

Jambeck, J. R., Geyer, R., Wilcox, C., Siegler, T. R., Perryman, M., Andrady, A., Narayan, R., and Law. K. L. (2015). "Plastic waste inputs from land into ocean," *Science* 347 (6223), 768-771. DOI: 10.1126/science.1260352

Jeswiet, J., Micari, F., Hirt, G., Bramley, A., Duflou, J., and Allwood, J. (2005). "Asymmetric single point incremental forming of sheet metal," *CIRP Annals* 54 (2), 88-114. DOI: 10.1016/S0007-8506(07)60021-3

Lebreton, L., Slat, B., Ferrari, F., Sainte-Rose, B., Aitken, J., Marthouse, R., Hajbane, S., Cunsolo, S., Schwarz, A., Levivier, A., *et al*. (2018). "Evidence that the Great Pacific Garbage Patch is rapidly accumulating plastic," *Nature, Scientific Reports* 8:4666. DOI: 10.1038/s41598-018-22939-w

Leminen, V., Tanninen, P., Mäkelä, P., and Varis, J. (2013). "Combined effect of paperboard thickness and mould clearance in the press forming process," *BioResources* 8 (4), 5701-5714. DOI: 10.15376/biores.8.4.5701-5714

Linvill, E., and Östlund, S. (2016). "Parametric study of hydroforming of paper materials using the explicit finite element method with a moisture-dependent and temperature-dependent constitutive model," *Packaging Technology and Science* 29, 145-160. DOI: 10.1002/pts.2193

Lohse, H., Weber, J., Heiduser, S., Hauptmann, M., Majschak, J.-P., Enz, B., and Helbig, A. (2010). "Pulling of paper and carton: Electrohydraulic drive system enables a flexible process design," *Ölhydraulik und Pneumatik* 5, 192-196.

Löwe, A., Hauptmann, M., and Majschak, J.-P. (2017a). "The effect of ultrasonic oscillation on the quality of 3D shapes during deep-drawing of paperboard," *BioResources* 12(4), 7178-7194. DOI: 10.1063/1.5034948

Löwe, A., Hofmann, A., Hauptmann, M. (2017b). "The use and application of ultrasonic vibrations in the 3D deformation of paper and cardboard," *Journal of Materials Processing Technology* 240, 23-32. DOI: 10.1016/j.jmatprotec.2016.09.006

Merkl, A., Stuchtey, M., Russel, S., Crow, A., Simon, E., Wooster, J., and Erdmann, H. (2015). *Stemming the Tide: Land-based Strategies for a Plastic-free Ocean*, Ocean Conservancy and McKinsey Center for Business and Environment, (https://oceanconservancy.org/wp-content/uploads/2017/04/full-report-stemming-the.pdf).

Micari, F., Ambrogio, G., and Filice, L. (2007). "Shape and dimensional accuracy in Single Point Incremental Forming: State of the art and future trends," *Journal of Materials Processing Technology,* 390-395. DOI: 10.1016/j.jmatprotec.2007.03.066

Müller, T., Lenske, A., Hauptmann, M., and Majschak, J.-P. (2017). "Analysis of dominant process parameters in deep drawing of paperboard," *BioResources* 12(2), 3530-3545. DOI: 10.15376/biores.12.2.3530-3545

Nazhad, M. M., Harris, E. J., Dodson, C. T. J., and Kerekes, R. J. (2000). "The influence of formation on tensile strength of paper made from mechanical pulps," *Tappi Journal* 83(12), 63-72.

Neto, D. M., Martins, J. M. P., Oliveira, M. C., Menezes, L. F., and Alves, J. L. (2015). "Evaluation of strain and stress states in the single point incremental forming process," *The International Journal of Advanced Manufacturing Technology* 85 (1-4), 521-534. DOI: 10.1007/s00170-015-7954-9

Östlund, M. (2005). *Residual Stresses in Paperboard and the Influence of Drying Conditions*, Ph.D. Dissertation, Kungliga Tekniska Högskolan, Stockholm.

Post, P.-P., Huttel, D., Groche, P., and Schabel, S. (2011). "Paper characteristics influencing the deep drawing ability of paper," in: *Progress in Paper Physics Seminar*, Graz, Austria.

Pflug, J., Xinyu, F., Lavalaye, J., Verpoest, I., Bratfisch, P., and Vandepitte, D. (2002). "Continously produced honeycomb sandwich materials for automotive applications," at *Automotive and Transportation Technology Congress and Exposition*. DOI: 10.4271/2002-01-1272

Putz, H.-J. (2013). "Recovered paper, recycled fibers," in: *Handbook of Paper and Board*, H. Holik (ed.), Weinheim, Germany. ISBN: 978-3-527-65252-5

Rhim, J.-W., Lee, J.-H., and Hong, S.-I. (2006). "Water resistance and mechanical properties of biopolymer (alignate and soy protein) coated paperboards," *LWT - Food Science and Technology* 39 (7), 806-813. DOI: 10.1016/j.lwt.2005.05.008

Rhim, J.-W., Lee, J.-H., and Hong, S.-I. (2007). "Increase in water resistance of paperboard by coating with poly(lactide)," *Packaging Technology and Science* 20, 393-402. DOI: 10.1002/pts.767

Rhim, J.-W. (2010). "Effect of moisture content on tensile properties of paper-based food packaging materials," *Food Science and Biotechnology* 19 (1), 243-247. DOI: 10.1007/s10068-010-0034-x

Salmén, L. (1993). "Responses of paper properties to changes in moisture content and temperature," *Products of Papermaking* 1, 369-430.

Schabel, S. (2017). "Bauen mit Papier," *Wochenblatt für Papierfabrikation* 145 (12), 822-825.

Scherer, K. (1935). *Das Ziehen von Pappe: Untersuchungen über die Ziehfähigkeit und den Ziehvorgang von Pappe*, Papier-Zeitung Verlagsgesellschaft mbH, Berlin, Germany.

Sridach, W., Hodgson, K. T., and Nazhad, M. M. (2006). "Biodegradation and recycling potential of barrier coated paperboards," *BioResources* 2(2), 179-192. DOI: 10.15376/biores.2.2.179-192

Stein, P., Franke, W., Hoppe, F., Hesse, D., Mill, K., and Groche, P. (2017). "Control of anisotropic shape deviation in single point incremental forming of paperboard," in: *AIP Conference Proceedings of the ESAFORM Conference*, Dublin, Ireland, 1896, 080007. DOI: 10.1063/1.5008087

Stein, P., Mushövel, J., Franke, W., and Groche, P. (2018). "Increased formability of paperboard by hydrostatic pressure," in: *Progress in Paper Physics Seminar*, Lodz, Poland.

Tanninen, P., Kasurinen, M., Eskelinen, H., Varis, J., Lindell, H., Leminen, V., Matthews, S., and Kainusalmi, M. (2014). "The effect of tool heating arrangement on fibre material forming," *Journal of Material Processing Technology* 214, 1576-1582. DOI: 10.1016/j.jmatprotec.2014.03.001

Tanninen, P., Leminen, V., Kainusalmi, M., and Varis, J. (2016). "Effect of process parameter variation on the dimensions of press-formed paperboard trays," *BioResources* 11(1), 140-158. DOI: 10.15376/biores.11.1.140-158

Tanninen, P. (2015). *Press Forming of Paperboard – Advancement of Converting Tools and Process Control*, Ph.D. Dissertation, Lappeenranta University of Technology, Lappeenranta, Finland.

Umweltbundesamt (Federal Environment Agency) (2016). "Verwertung von Kunststoffabfällen," (https://www.umweltbundesamt.de/daten/ressourcen-abfall/verwertung-entsorgung-ausgewaehlter-abfallarten/kunststoffabfaelle#textpart-1), accessed 03 July 2018.

Vainio, A., and Paulapuro, H. (2007). "The effect of wet pressing and drying on bonding and activation in paper," *Nordic Pulp and Paper Research Journal* 22(4), 403-408.

Vishtal, A., and Retulainen, E. (2012). "Deep-drawing of paper and paperboard: The role of material properties," *BioResources* 7(3), 4424-4450. DOI: 10.15376/biores.7.3.4424-4450

Wallmaier, M., Noack, K., Hauptmann, M., and Majschak, J.-P. (2016). "Shape accuracy analysis of deep drawn packaging components made of paperboard," *Nordic Pulp and Paper Research Journal* 31(2), 323-332. DOI: 10.3183/NPPRJ-2016-31-02-p323-332

Yajima, M., Ishii, M., and Kobayashi, M. (1970). "The effects of hydrostatic pressure on the ductility of metals and alloys," *International Journal of Fracture Mechanics* 6 (2), 139-150.

Article submitted: September 20, 2018; Peer review completed: December 15, 2018; Revised version received and accepted: December 30, 2018; Published: January 15, 2019
DOI: 10.15376/biores.14.1.1731-1764